



Brigham Young University
BYU ScholarsArchive

Theses and Dissertations

2002-05-31

Elasticity in Microstructure Sensitive Design Through the use of Hill Bounds

Benjamin L. Henrie
Brigham Young University - Provo

Follow this and additional works at: <https://scholarsarchive.byu.edu/etd>

 Part of the Mechanical Engineering Commons

BYU ScholarsArchive Citation

Henrie, Benjamin L., "Elasticity in Microstructure Sensitive Design Through the use of Hill Bounds" (2002).
Theses and Dissertations. 94.
<https://scholarsarchive.byu.edu/etd/94>

This Thesis is brought to you for free and open access by BYU ScholarsArchive. It has been accepted for inclusion in Theses and Dissertations by an authorized administrator of BYU ScholarsArchive. For more information, please contact scholarsarchive@byu.edu, ellen_amatangelo@byu.edu.

ELASTICITY IN MICROSTRUCTURE SENSITIVE DESIGN THROUGH
THE USE OF HILL BOUNDS

by

Benjamin L. Henrie

A thesis submitted to the faculty of

Brigham Young University

in partial fulfillment of the requirements for the degree of

Master of Science

Department of Mechanical Engineering

Brigham Young University

August 2002

BRIGHAM YOUNG UNIVERSITY

GRADUATE COMMITTEE APPROVAL

of a thesis submitted by

Benjamin L. Henrie

This thesis has been read by each member of the following graduate committee and by majority vote has been found to be satisfactory.

Date

Brent L. Adams, Chair

Date

Larry L Howell

Date

Tracy W. Nelson

BRIGHAM YOUNG UNIVERSITY

As chair of the candidate's graduate committee, I have read the thesis of Benjamin L. Henrie in its final form and have found that (1) its format, citations, and bibliographical style are consistent and acceptable and fulfill university and department style requirements; (2) its illustrative materials including figures, tables, and charts are in place; and (3) the final manuscript is satisfactory to the graduate committee and is ready for submission to the university library.

Date

Brent L. Adams, Chair

Accepted for the Department

Larry L Howell
Department Chair

Accepted for the College

Douglas M Chabries
Dean, College of Engineering and Technology

ABSTRACT

ELASTICITY IN MICROSTRUCTURE SENSITIVE DESIGN THROUGH THE USE OF HILL BOUNDS

Benjamin L. Henrie

Department of Mechanical Engineering

Master of Science

In engineering, materials are often assumed to be homogeneous and isotropic; in actuality, material properties do change with sample direction and location. This variation is due to the anisotropy of the individual grains and their spatial distribution in the material. Currently there is a lack of communication between the design engineer, material scientist, and processor for solving multi-objective/constrained designs. If communication existed between these groups then materials could be designed for applications, instead of the reverse. Microstructure sensitive design introduces a common language, a spectral representation, where both design properties and microstructures are expressed.

Using Hill bounds, effective elastic properties are expressed within the spectral representation. For the elastic properties, two FCC materials, copper and nickel, were

chosen for computation and to demonstrate how symmetry enters into the methodology. This spectral representation renders properties as hyper-surfaces that translate through a multi-dimensional Fourier space depending on the property value of the hyper-surface. Property closures are generated by condensing the information contained within the multi-dimensional Fourier space into a 2-D representation. This compaction of information is beneficial for a quick determination of property limits for a particular alloy system. The design engineer can now dictate the critical design properties and receive sets of microstructures that satisfy the design objectives.

ACKNOWLEDGMENTS

This research was supported by funding from the army research office (ARO). This assistance is gratefully acknowledged.

I would like to thank Dr. Brent L. Adams for the many hours he has spent going over theory and encouragement. I want to especially thank him for the opportunity to work with him and his research team. He has greatly influenced my path through schooling, and through out my life.

I also want to thank my graduate committee, Dr. Nelson and Dr. Howell.

I would like to thank my parents for helping me to have the dream to pursue my education and their financial help in the beginning. They have been a source of encouragement even when they thought that I would never finish.

My wife has been wonderful through the entire experience. Alisa has forever changed the way my life is headed: First by marrying me and then by redirecting my degree from Electrical Engineering to Mechanical Engineering. She is responsible for starting my undergraduate research with Dr. Adams and encouraging me when life was hard. She is the best thing that has ever happened to me.

Table of Contents

List of Figures	ix
List of Tables	xi
1 Introduction.....	1
1.1 Overview.....	1
1.2 History of Microstructure Sensitive Design	2
1.3 Elasticity	4
2 Local State Space.....	7
2.1 Overview.....	7
2.2 Local States.....	7
2.3 Local State Space.....	8
2.4 Basis Functions	9
2.5 Fourier Representation of the Local State Space.....	10
2.6 Microstructure Hull.....	11
3 Elasticity, Hill Bounds.....	13
3.1 Overview.....	13
3.2 Elastic Homogenization Relations.....	13
3.3 Fourier Representation of the Upper Bound.....	15
3.4 Fourier Representation of the Lower Bound	18
3.4.1 Inversion of the Lower Bound	20
4 Alloy System.....	23
4.1 Overview.....	23
4.2 Elastic Bounds with Crystal and Sample Symmetry	23
5 Elastic Properties in Fourier Space	29
5.1 Overview.....	29
5.2 Hyper-Surfaces in the Fourier Space	29

5.3	Extraction of Microstructures from the Fourier Space	33
6	Property Closures.....	35
6.1	Overview.....	35
6.2	Generation of the Property Closures.....	35
6.3	Benefits of the Property Closures	36
7	Conclusions and Recommendations	39
7.1	Conclusions.....	39
7.2	Recommendations.....	40
	References.....	41
	Appendix.....	45
	Appendix A : Property Closures.....	45
	Appendix B : Inversion for cubic-orthorhombic symmetry	52
	Appendix C :Program for generation of the property closures.....	54
	Appendix D : Program for generation of the upper-bound.....	57
	Appendix E : Program for generation of the lower-bound	59
	Appendix F : Program for computing the $\phi D_{lr}^{*l\eta}$ coefficients.....	63
	Appendix G : Harmonics.h subroutine	65
	Appendix H : Property.h subroutine	76

List of Figures

Figure 1.1 Ashby chart of youngs modulus vs. strength (Ashby, 1992)	2
Figure 1.2 MSD paradigm –new approach.....	4
Figure 2.1 Piecewise constant function	10
Figure 2.2 Cubic-orthorhombic microstructure hull.....	12
Figure 3.1 Elastic constants of Cu-Ni alloys for values predicted by Hartley and those obtained from experiments. Hartley (2001).....	17
Figure 4.1 Copper-Nickel alloy system	24
Figure 4.2 Number of linearly independent spherical harmonics of different symmetries as a function of degree l (for even l). (Bunge1982).....	26
Figure 4.3 Number of linearly independent spherical harmonics of different symmetries as a function of degree l (for odd l). (Bunge 1982)	26
Figure 5.1 Elastic upper-bound of $\langle C_{1111} \rangle$ and $\langle C_{1212} \rangle$ in the microstructure hull....	30
Figure 5.2 Elastic lower-bound of the hyper-surface $\langle S \rangle_{1111}^{-1}$ in the microstructure hull	32
Figure 5.3 Microstructure hull with $\langle S \rangle_{1111}^{-1}$ and $\langle C_{1212} \rangle$ hyper-surfaces. The area in yellow contains those microstructures that fulfill the design constraints.	33
Figure 5.4 One extracted microstructure that satisfy both the $\langle S \rangle_{1111}^{-1}$ and $\langle C_{1212} \rangle$ bounds.....	34
Figure 6.1 Property closure of C_{1111}^* vs. C_{1212}^* of the Cu-Ni alloy system.....	37
Figure 6.2 Property closure of C_{1111}^* vs. C_{1212}^* with design constraints added at A and B	37
Figure A.1 Property closure of C_{1111}^* vs. C_{2222}^*	45
Figure A.2 Property closure of C_{1111}^* vs. C_{3333}^*	45
Figure A.3 Property closure of C_{1111}^* vs. C_{2323}^*	46

Figure A.4 Property closure of C_{1111}^* vs. C_{3131}^*	46
Figure A.5 Property closure of C_{2222}^* vs. C_{3333}^*	47
Figure A.6 Property closure of C_{2222}^* vs. C_{2323}^*	47
Figure A.7 Property closure of C_{2222}^* vs. C_{3131}^*	48
Figure A.8 Property closure of C_{2222}^* vs. C_{1212}^*	48
Figure A.9 Property closure of C_{3333}^* vs. C_{2323}^*	49
Figure A.10 Property closure of C_{3333}^* vs. C_{3131}^*	49
Figure A.11 Property closure of C_{3333}^* vs. C_{1212}^*	50
Figure A.12 Property closure of C_{2323}^* vs. C_{3131}^*	50
Figure A.13 Property closure of C_{2323}^* vs. C_{1212}^*	51
Figure A.14 Property closure of C_{3131}^* vs. C_{1212}^*	51

List of Tables

Table 3.1 Transforming from four indices, S_{ijkl} , to two indices, S_{ij}	21
Table 5.1 $D_l^{1\mu}$ coefficients for the cubic-orthorhombic case for the on-diagonal elements	31

1 Introduction

1.1 Overview

In engineering, materials are assumed to be homogeneous and isotropic; in actuality, material properties do change with sample direction and location. This variation is due to the anisotropy of the individual grains and their spatial distribution in the material. This thesis will develop the basic methodology of Microstructure Sensitive Design, through the use of elastic bounds (Hill bounds), and demonstrate how microstructures can be used as a design parameter.

Charts, such as Ashby charts (Figure 1.1, Ashby, 1992), have been compiled to show property limits of the generic materials database, but these charts do not take into account the microstructure of the material. If microstructure and composition are taken into account, more property variance is predicted.

With highly constrained design, e.g. space shuttle, the design engineer may discover that there are no materials that will satisfy the design objectives. Typically design materials are selected first for design work, but if the material is a design variable than great design freedom can be achieved.

The traditional approach for material insertion is Material Scientist → Processor → Design Engineering. Scientists and Processing Engineers try to develop materials with improved properties to impart to the Design Engineers. If the new material has

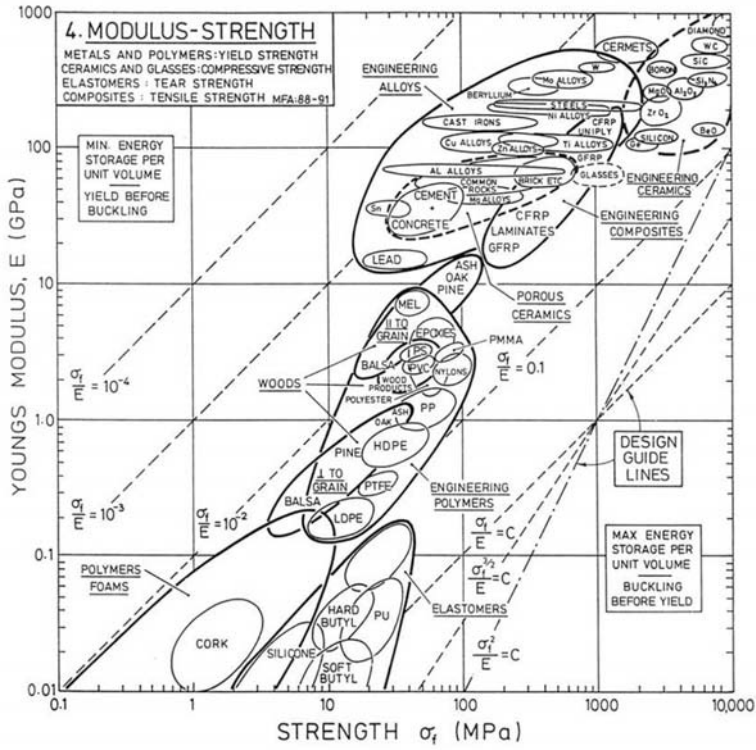


Figure 1.1 Ashby chart of youngs modulus vs. strength
(Ashby, 1992)

properties that fulfill the design constraints then the engineer can design with this new material. Within the traditional approach there exists no common language between groups to facilitate the development of improved materials.

1.2 History of Microstructure Sensitive Design

In an effort to unite Design Engineers, Material Scientists, and Processors Engineers together, a new approach has been developed called Microstructure Sensitive Design (MSD). The goal of MSD is to improve material performance through the creation of a common language within the traditional approach.

The concept of improving material properties through microstructure is not new. Using varying techniques, ways to overcome generic material limitations are being

developed. Larsen (et al., 1997) used topology optimization to find microstructures that exhibit negative poison's ratios for compliant micro-mechanisms. Design of piezocomposites by the same method was performed by Sigmund (et al., 1998). Olhoff (et al., 1998) extended these methods to consider three-dimensional elastic continuum structures. Olsen (1998) and Subbarayan and Raj (1999) have proposed methods of integrating material science with engineering to improve the development of new materials.

Adams (et al., 2001) proposed a spectral approach of microstructure design to meet multi-objective/constrained designs, which this work builds upon. The new approach, Figure 1.2, adds an additional element that creates a common language for communication. Within this spectral representation the complete microstructure, design properties, and processing paths can be expressed. This thesis does not focus on the problem of finding the optimal microstructure for one application, but shows the combined elastic limits that the Cu-Ni alloy system can achieve through variations in composition and microstructure.

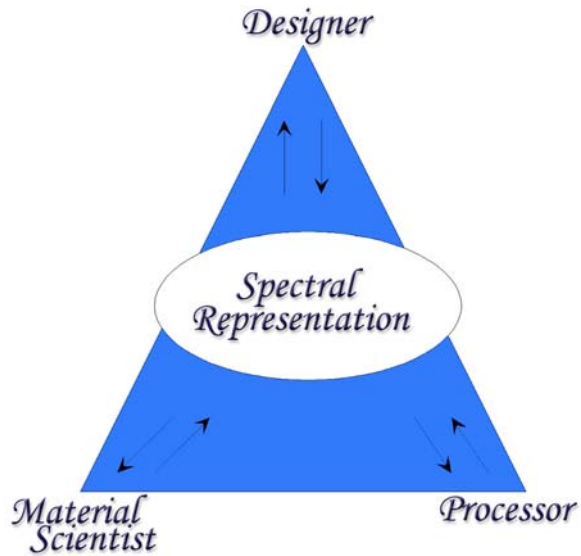


Figure 1.2 MSD paradigm –new approach

1.3 Elasticity

One material property of importance to many designs is elasticity. For example beam deflection, as required in compliant mechanisms (Howell, 2001), depends on this material property. The prediction of elastic properties has been a recurring undertaking in the literature. Voigt (1928) proposed to estimate the elastic moduli by the assumption that strain is uniform throughout an aggregate. Reuss (1929) proposed to estimate the elastic moduli using the assumption that stress is uniform throughout an aggregate. Hill (1952) demonstrated that the Voigt and Reuss averages had produced upper and lower bounds to the measured elastic moduli. Hashin and Shtrikman (1962a, 1962b), using a variation principle, developed narrower bounds than those obtained by the Voigt and Reuss averages. Beran (et al., 1996) adapted the Hashin and Shtrikman variational principle to obtain improved bounds for the effective stiffness tensor in orthotropic materials.

In the present work the Hill bounds are used to produce combined elastic properties closures for the Cu-Ni system covering the complete range of composition and microstructure. These closures permit an engineer to identity if the Cu-Ni system satisfies the required elasticity for a design. Additionally the Hill bounds are expressed as a Fourier series for use in the spectral representation.

2 Local State Space

2.1 Overview

Before properties can be expressed within the common language, the spectral representation must be defined. The local states space is defined on the premise that salient local properties are dependent upon a small number of local state variables. The local state space is a collection of all possible local states. This state space is later translated into a set of Dirac functions in the Fourier space. Weighted combinations of these Dirac functions will be used to represent all possible microstructures on the local state space. Representation of the local state space and the set of all possible microstructures in their Fourier components constitutes the spectral representation.

2.2 Local States

The basic premise behind MSD is that salient local properties, p_i , are dependent upon a small number of local state variables, h , that are presumed known to the observer,

$$p_i = p_i(h). \quad (2.1)$$

Local states can be crystal orientation, composition, reference shear stress for dislocation slip, and others. Through homogenization relationships the local properties, and their distribution in the microstructure, are linked with estimated effective (macroscopic) properties (Chapter 3).

In this work three local state variables are employed

$$h = (\phi, g, \lambda), \quad (2.2)$$

where ϕ is phase, g is lattice orientation, and λ is composition. These local state variables belong to the sets $\phi \in \{1, 2, 3, \dots, n\} = \Phi$, $g \in SO(3) / {}^\phi G = {}^\phi \Gamma$, and $\lambda \in [0, 1] = \Lambda$. $SO(3)$ is the 3-dimensional special orthogonal group of rotations of the crystal lattice, and ${}^\phi G$ is the crystallographic symmetry subgroup of phase ϕ . Thus, ${}^\phi \Gamma$ represents the set of all physically distinctive orientations of the crystal lattice associated with phase ϕ (Adams and Olson 1998). λ represents composition for this work, but λ can be utilized for any scalar parameter.

2.3 Local State Space

The local state space, H , shall consist of all possible (ordered) sets of local state variables. Local state is defined as one element of the local state space. If only a single phase material is considered then

$$h \in H = {}^\phi \Gamma \times \Lambda. \quad (2.3)$$

If the material is a two phase system then

$$h \in H = ({}^1 H \cup {}^2 H). \quad (2.4)$$

where ${}^1 H$ and ${}^2 H$ are defined by

$${}^\phi H = {}^\phi \Gamma \times \Lambda. \quad (2.5)$$

2.4 Basis Functions

Following Bunge (1982), the classical crystal symmetric generalized spherical harmonic functions, $T_l^{mn}(g)$, are used to represent the orientation dependence on ${}^\phi\Gamma$. The crystal symmetric basis functions, ${}^\phi\dot{T}_l^{\mu\nu}(g)$, are special linear combinations of the generalized spherical harmonic functions,

$${}^\phi\dot{T}_l^{\mu\nu}(g) = \sum_{m=-l}^{+l} \sum_{n=-l}^{+l} {}^\phi\dot{A}_l^{m\mu} {}^\phi\dot{A}_l^{n\nu} T_l^{mn}(g). \quad (2.6)$$

The symmetry coefficients, ${}^\phi\dot{A}_l^{m\mu}$, carry the crystal symmetry and the coefficients, ${}^\phi\dot{A}_l^{n\nu}$, carry the sample symmetry. The $T_l^{mn}(g)$ functions form a complete system of orthonormal functions with the following property:

$$\int_{{}^\phi\Gamma} T_l^{mn}(g) T_l^{*mn}(g) dg = \frac{1}{2l+1} \delta_{ll'} \delta_{mm'} \delta_{nn'}, \quad (2.7)$$

where * is the complex conjugate.

Piecewise constant functions are used to provide the basis for composition dependence on Λ . $\chi_r(\lambda)$ are defined to be piecewise constant functions (Keener, 2000) defined on subintervals of the range of λ_r (as enumerated by the index r), as shown in Figure 2.1. Thus,

$$\chi_r(\lambda) = \begin{cases} 1/M(\lambda_r) & \text{if } \lambda \in \lambda_r \\ 0 & \text{otherwise} \end{cases}. \quad (2.8)$$

These form a complete system of orthonormal functions

$$\int_{\lambda_r} \chi_r(\lambda) \chi_{r'}(\lambda) d\lambda = \frac{\delta_{rr'}}{M(\lambda_r)}, \quad (2.9)$$

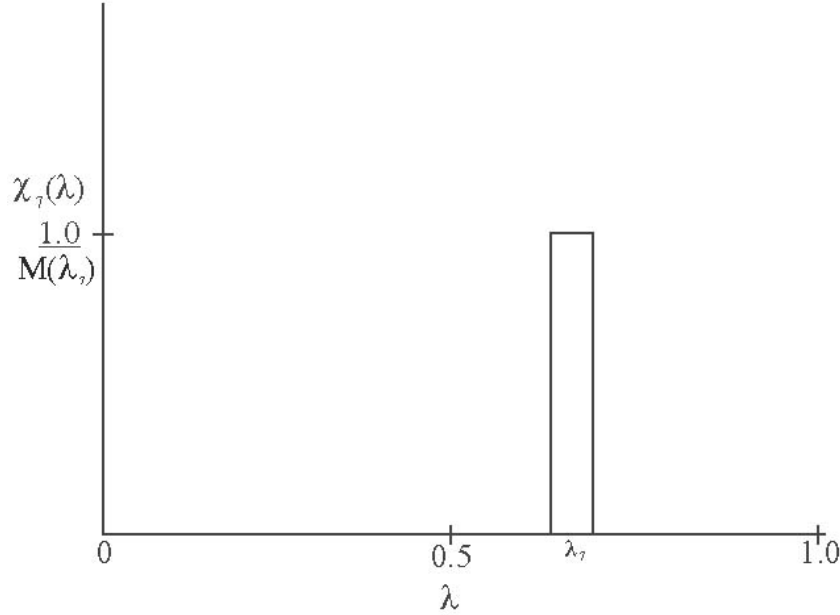


Figure 2.1 Piecewise constant function

where $M(\lambda_r)$ is the measure of λ_r . (Note: exponential and other types of functions could also be used as a basis for representing scalar parameters.)

2.5 Fourier Representation of the Local State Space

Transforming the local state space into its Fourier basis requires transforming H into an equivalent space, H' . This transformation is performed by expressing each possible local state, say h_j , as a Dirac function, defined here in the conventional way:

$$\int_{H'} \delta(h - h_j) dh = \begin{cases} 1 & \text{if } h_j \in H' \\ 0 & \text{otherwise} \end{cases}. \quad (2.10)$$

The Dirac function is then expressed in a Fourier series

$$\delta(h - h_j) = \sum_{\phi=1}^n \sum_{l=0}^{\infty} \sum_{m=-l}^{+l} \sum_{n=-l}^{+l} \sum_{r=1}^{N_\Lambda} \phi F_{lr}^{mn} T_l^{mn}(g_j) \chi_r(\lambda_j). \quad (2.11)$$

From relations (2.7) and (2.9), the Fourier coefficients of the Dirac function have the form

$${}^\phi F_{lr}^{mn} = (2l+1) M(\lambda_j) T_l^{*mn}(g_j) \chi_r(\lambda_j). \quad (2.12)$$

2.6 Microstructure Hull

For the homogenization relations of interest in Chapter 3, microstructure is specified by the local state distribution function, $f(h)$, which defines the volume fraction dV/V of sample volume that lies within a range dh of local state h :

$$\frac{dV}{V} = f(h)dh. \quad (2.13)$$

Here dh is the invariant measure (see Bunge, 1982). The local state distribution function, $f(h)$, is normalized, as can be seen from equation (2.13), according to

$$\int f(h) dh = 1 \quad (2.14)$$

and expressed as a series of generalized spherical harmonics functions (Courant and Hilbert, 1989),

$$f(h) = \sum_{l=0}^{\infty} \sum_{n=-l}^{+l} \sum_{m=-l}^{+l} \sum_{r=1}^{N_A} {}^\phi F_{lr}^{mn} T_l^{mn}(g) \chi_r(\lambda). \quad (2.15)$$

It is convenient to represent $f(h)$ as a summation of Dirac functions, weighted by the appropriate volume fractions, ν_j ,

$$f(h) = \sum_{j=1}^N \nu_j \delta(h - h_j). \quad (2.16)$$

The set of volume fractions, ν_j , are constrained to sum to one:

$$\sum_j \nu_j = 1. \quad (2.17)$$

This local state distribution resides in an infinite-dimensional Fourier space, although the homogenization relations introduced in Chapter 3 require only finite-dimensional approximations of $f(h)$.

The set of all possible $f(h)$ is called the microstructure hull; it consists of all possible microstructures pertinent to the chosen homogenization relations and local state space. Formally, the microstructure hull, as described in the Fourier space, obtained from relations (2.11, 12, and 14) when constrained by (2.15) (see Adams *et al.* 2001). Graphically, this microstructure hull is difficult to view because of the infinite-dimensional nature of the Fourier space in which it resides; however for the homogenization relations (Hill bounds) of interest in this thesis (Chapter 3), with cubic-orthorhombic symmetry, the pertinent part of the Fourier space reduces to three dimensions, as seen in Figure 2.2.

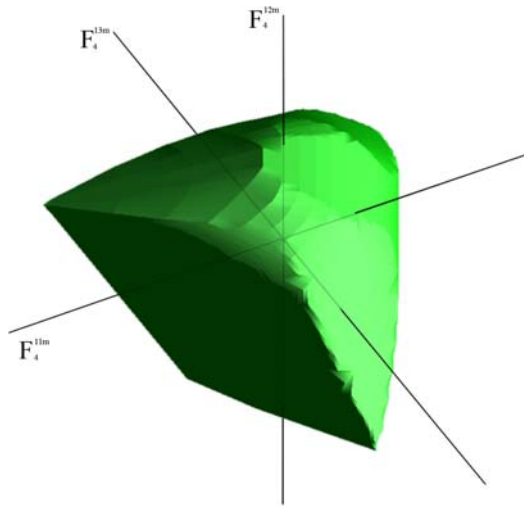


Figure 2.2 Cubic-orthorhombic microstructure hull

3 Elasticity, Hill Bounds

3.1 Overview

The design engineer's input into MSD is to specify the significant effective properties. By specifying the local properties, the designer makes certain that microstructures are chosen that fulfill the design objectives. Through the use of elastic homogenization relationships the effective elastic properties are linked with the local elastic properties, and their distribution in the microstructure. Using work performed by Hill (1952) the effective elastic properties are estimated through upper and lower bounds. These bounds are then represented by a series of basis functions described in section 2.4. For this chapter, consideration of symmetry is omitted to simplify the general overview of the theoretical development.

3.2 Elastic Homogenization Relations

The stiffness tensor, C_{ijkm} ¹, relates stress to strain by Hooke's law

$$\sigma_{ij} = C_{ijkm} \varepsilon_{km} . \quad (3.1)$$

Here σ_{ij} is the stress tensor, and ε_{km} is the strain tensor. The compliance tensor, S_{ijkm} , is derived from the stiffness tensor by

¹ Repeated indices implies summation over the integers 1,2,3 according to the Einstein summation convention, except as otherwise noted.

$$C_{ijkm} S_{kmpq} = \frac{1}{2} [\delta_{ip} \delta_{jq} + \delta_{iq} \delta_{jp}] \quad (3.2)$$

where δ_{ip} is the Kronecker Delta². Compliance is defined by the relation

$$\varepsilon_{ij} = S_{ijkm} \sigma_{km}. \quad (3.3)$$

Hill (1952) demonstrated that the Voigt and Reuss averages were really upper and lower elastic bounds. Following Hill, we define the effective stiffness, C_{ijkm}^* , as

$$\langle \sigma_{ij} \rangle = C_{ijkm}^* \langle \varepsilon_{km} \rangle, \quad (3.4)$$

where $\langle \cdot \rangle$ denotes volume average quantities. The effective tensor is determined from knowledge of the single crystal tensor and the statistical properties of the microstructure. Compliance has a similar effective tensor.

Beran (1996) showed that the upper and lower bounds of the effective tensor can be calculated through two classical variational principles: the principle of minimum potential energy, and the principle of complementary energy. These principles for the effective stiffness tensor form lower and upper bounds

$$\langle \varepsilon_{ij} \rangle \langle S \rangle_{ijkm}^{-1} \langle \varepsilon_{km} \rangle \leq \langle \varepsilon_{ij} \rangle C_{ijkm}^* \langle \varepsilon_{km} \rangle \leq \langle \varepsilon_{ij} \rangle \langle C_{ijkm} \rangle \langle \varepsilon_{km} \rangle. \quad (3.5)$$

A similar expression for S_{ijkm}^* can be derived.

Evaluation of (3.5) does not directly provide bounds for all components of C_{ijkm}^* . Direct bounds obtained only for C_{iiii}^* (no sum on i) and C_{ijij}^* (no sum on i or j, $i \neq j$). Bounds can be found for off diagonal elements, but some additional work is required. This thesis will focus on bounds for the “on-diagonal” cases.

² The Kronecker Delta function is expressed as $\delta = \begin{cases} 1 & \text{if } (i=p) \\ 0 & \text{if } (i \neq p) \end{cases}$

3.3 Fourier Representation of the Upper Bound

Equation (3.5) for the upper bound can be expressed in terms of the local state density function as

$$\langle C_{ijkl} \rangle = \sum_{\phi=1}^n \iiint_{SO(3)/{}^\phi G} \int_{\Lambda} f(\phi, g, \lambda) {}^\phi C_{ijkl}(g, \lambda) d\lambda dg \quad (3.6)$$

where dg is the invariant measure in orientation space, $\sin(\theta) d\varphi_1 d\theta d\varphi_2$, and $\varphi_1, \theta, \varphi_2$ are the Euler angles defined by Bunge(1982). Both $f(\phi, g, \lambda)$ and ${}^\phi C_{ijkl}(g, \lambda)$ are real-valued functions on the local state space, H .

Since ${}^\phi C_{ijkl}(g, \lambda)$ is the elastic stiffness tensor in the sample coordinate frame a relationship must be found to relate ${}^\phi C_{ijkl}(g, \lambda)$ with the elastic stiffness tensor in the crystal coordinate frame, ${}^\phi C_{ijkl}^\circ(\lambda)$. This relationship is required because the elastic constants, i.e. ${}^\phi C_{11}^\circ(\lambda)$, ${}^\phi C_{12}^\circ(\lambda)$, ${}^\phi C_{44}^\circ(\lambda)$ (Hirth and Lothe 1968), are measured in the crystal coordinate frame. ${}^\phi C_{ijkl}^\circ(\lambda)$ is

$${}^\phi C_{ijkl}^\circ(\lambda) = {}^\phi C_{12}^\circ(\lambda) \delta_{ij} \delta_{km} + {}^\phi C_{44}^\circ(\lambda) [\delta_{ik} \delta_{jm} + \delta_{im} \delta_{jk}]. \quad (3.7)$$

Using the “passive” notation³, as used by Bunge (1982), the direction cosines, g_{ij} , are defined as

$$e_i = g_{ij} e_j^\circ. \quad (3.8)$$

The rotation from the crystal frame to the sample frame is performed as

³ The passive notation is of the form $f(g_\phi \circ g) = f(g)$ where g transforms a sample fixed coordinate system, K_a into a crystal fixed coordinate system K_b . g_ϕ is a rotation that transforms a crystal from one orientation to a symmetrically equivalent orientation.

$${}^\phi C_{abcd}(g, \lambda) = g_{ai}g_{bj}g_{ck}g_{dm} {}^\phi C_{ijkm}^\circ(\lambda). \quad (3.9)$$

For cubic symmetry (3.9) can be written in a simpler form as

$$\begin{aligned} {}^\phi C_{ijkm}(g, \lambda) = & {}^\phi C_{12}^\circ(\lambda)\delta_{ij}\delta_{km} + {}^\phi C_{44}^\circ(\lambda)[\delta_{ik}\delta_{jm} + \delta_{im}\delta_{jk}] + \\ & [{}^\phi C_{11}^\circ(\lambda) - {}^\phi C_{12}^\circ(\lambda) - 2{}^\phi C_{44}^\circ(\lambda)]g_{ri}g_{rj}g_{rk}g_{rm} \end{aligned} \quad (3.10)$$

The relationship $g_{ri}g_{rj}g_{rk}g_{rm}$ implies a summation over r from 1 to 3:

$$g_{ri}g_{rj}g_{rk}g_{rm} = g_{1i}g_{1j}g_{1k}g_{1m} + g_{2i}g_{2j}g_{2k}g_{2m} + g_{3i}g_{3j}g_{3k}g_{3m} \quad (3.11)$$

Hartley (2001) describes a method for finding the material constants, ${}^\phi C_{ij}^\circ(\lambda)$, for a homogenous composition of two materials. Figure 3.1 shows Hartley's predictions for the material constants of the Cu-Ni alloy system, and their comparison to measured values.

Relation (3.10) is divided into two parts

$${}^\phi A_{ijkm} = {}^\phi C_{12}^\circ(\lambda)\delta_{ij}\delta_{km} + {}^\phi C_{44}^\circ(\lambda)[\delta_{ik}\delta_{jm} + \delta_{im}\delta_{jk}] \quad (3.12)$$

and

$${}^\phi Z_{ijkm} = {}^\phi \beta(\lambda) g_{ri}g_{rj}g_{rk}g_{rm} \quad (3.13)$$

for a more simple transformation with basis functions. ${}^\phi \beta(\lambda)$ is given as

$${}^\phi \beta(\lambda) = {}^\phi C_{11}^\circ(\lambda) - {}^\phi C_{12}^\circ(\lambda) - 2{}^\phi C_{44}^\circ(\lambda) = \sum_{r=1}^{N_\Lambda} {}^\phi \beta_r \chi_r(\lambda). \quad (3.14)$$

Also, (3.12) is expressed using piecewise functions,

$${}^\phi A_{ijkm} = \sum_{r=1}^{N_\Lambda} {}^\phi k_r(ijkm) \chi_r(\lambda), \quad (3.15)$$

and (3.13) as a combination of piecewise and generalized spherical harmonic functions,

$${}^\phi Z_{ijkm} = \sum_{l=0}^4 \sum_{m=-l}^{+l} \sum_{n=-l}^{+l} \sum_{r=1}^{N_\Lambda} {}^\phi \beta_r {}^\phi D_l^{*mn}(ijkm) T_l^{*mn}(g) \chi_r(\lambda). \quad (3.16)$$

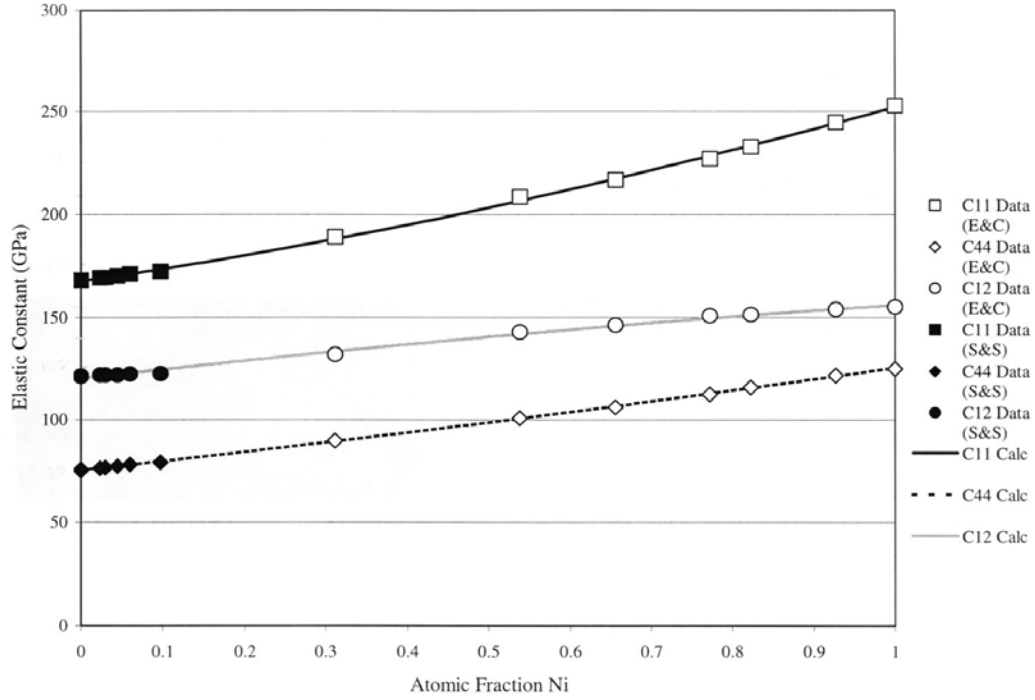


Figure 3.1 Elastic constants of Cu-Ni alloys for values predicted by Hartley and those obtained from experiments. Hartley (2001)

The two coefficients ${}^\phi\beta_r$ and ${}^\phi D_l^{*mn}(ijkm)$ maybe expressed as one coefficient, but the ${}^\phi D_l^{*mn}(ijkm)$ coefficients do not change with composition. From this property the ${}^\phi D_l^{*mn}(ijkm)$ coefficients are only calculated once for a set symmetry. The ${}^\phi\beta_r$ coefficients change for each alloy system, and require much less computational time.

Equation (3.16) shows that l needs to be enumerated only up to 4, due to the fact that it is the product of four direction cosines (Bunge, 1982):

$$g_{ri}g_{rj}g_{rk}g_{rm} = \sum_{l'=0}^4 \sum_{m'=-l}^{+l} \sum_{n'=-l}^{+l} {}^\phi D_l^{*m'n'}(ijkm) T_{l'}^{*m'n'}(g). \quad (3.17)$$

Combining (3.15) and (3.16), ${}^\phi C_{ijkm}$ becomes

$${}^\phi C_{ijkm} = \sum_{r=1}^{N_\Delta} {}^\phi k_r(ijkm) \chi_r(\lambda) + \sum_{l=0}^4 \sum_{m=-l}^{+l} \sum_{n=-l}^{+l} \sum_{r=1}^{N_\Delta} {}^\phi \beta_r {}^\phi D_l^{*mn}(ijkm) T_l^{*mn}(g) \chi_r(\lambda). \quad (3.18)$$

By combining equations (2.15), (3.6), and (3.18) the stiffness upper bound becomes

$$C_{ijkm}^* \leq \langle C_{ijkm} \rangle = \sum_{\phi=1}^n \sum_{l=0}^4 \sum_{m=-l}^{+l} \sum_{n=-l}^{+l} \sum_{r=1}^{N_\Delta} [{}^\phi k_r(ijkm) \delta_{l0} + {}^\phi \beta_r {}^\phi D_l^{*mn}(ijkm)] {}^\phi F_{lr}^{mn}. \quad (3.19)$$

From (3.19) the upper bound can be calculated for all pertinent microstructures and compositions. Note that the upper-bound relationship in (3.18) comprises, for fixed C_{ijkm}^* , a hyper-plane within the Fourier space. This hyper-plane consists of all Fourier components ${}^\phi F_{lr}^{mn}$, representing microstructures, which possess the same upper bound on effective stiffness.

3.4 Fourier Representation of the Lower Bound

The procedure for finding the elastic property closures for the lower bound is similar to the upper bound approach except for an inversion. From equation (3.5) the lower bound is

$$\langle S \rangle_{ijkm}^{-1}. \quad (3.20)$$

Before the inversion can be performed the average compliance tensor is computed from the local state distribution function:

$$\langle S_{ijkm} \rangle = \sum_{\phi=1}^n \iiint_{SO(3)/{}^\phi G} \int_{\Lambda} f(\phi, g, \lambda) {}^\phi S_{ijkm}(\lambda) d\lambda dg. \quad (3.21)$$

Relation (3.9) is changed to

$${}^\phi S_{abcd}(g, \lambda) = g_{ai} g_{bj} g_{ck} g_{dm} {}^\phi S_{ijkm}^\circ(\lambda), \quad (3.22)$$

where ${}^\phi S_{ijkm}^\circ$ is

$${}^\phi S_{ijkm}^\circ(\lambda) = {}^\phi S_{12}^\circ(\lambda)\delta_{ij}\delta_{km} + {}^\phi S_{44}^\circ(\lambda)(\delta_{ik}\delta_{jm} + \delta_{im}\delta_{jk}). \quad (3.23)$$

Equation (3.22) can be expressed in a simpler form for cubic symmetry as

$$\begin{aligned} {}^\phi S_{ijkm}(g, \lambda) = & {}^\phi S_{12}^\circ(\lambda)\delta_{ij}\delta_{km} + {}^\phi S_{44}^\circ(\lambda)[\delta_{ik}\delta_{jm} + \delta_{im}\delta_{jk}] + \\ & [{}^\phi S_{11}^\circ(\lambda) - {}^\phi S_{12}^\circ(\lambda) - 2{}^\phi S_{44}^\circ(\lambda)]g_{ri}g_{rj}g_{rk}g_{rm}. \end{aligned} \quad (3.24)$$

Hartley's method is again utilized (see section 3.3) for a homogenous composition of two materials. Equation (3.24) is broken up into two parts

$${}^\phi E_{ijkm} = {}^\phi S_{12}^\circ(\lambda)\delta_{ij}\delta_{km} + {}^\phi S_{44}^\circ(\lambda)[\delta_{ik}\delta_{jm} + \delta_{im}\delta_{jk}] \quad (3.25)$$

and

$${}^\phi Q_{ijkm} = {}^\phi \alpha(\lambda) g_{ri}g_{rj}g_{rk}g_{rm}, \quad (3.26)$$

where ${}^\phi \alpha$ is

$${}^\phi \alpha(\lambda) = {}^\phi S_{11}^\circ(\lambda) - {}^\phi S_{12}^\circ(\lambda) - 2{}^\phi S_{44}^\circ(\lambda) = \sum_{r=1}^{N_\Lambda} {}^\phi \alpha_r {}^\phi \chi_r(\lambda). \quad (3.27)$$

(3.25) is expressed with piecewise constant functions,

$${}^\phi E_{ijkm} = \sum_{r=1}^{N_\Lambda} {}^\phi k_r(ijkm) \chi_r(\lambda), \quad (3.28)$$

and (3.26) is a combination of piecewise and harmonic functions,

$${}^\phi Q_{ijkm} = \sum_{l=0}^4 \sum_{m=-l}^{+l} \sum_{n=-l}^{+l} \sum_{r=1}^{N_\Lambda} {}^\phi \alpha_r {}^\phi D_l^{*mn}(ijkm) T_l^{*mn}(g) \chi_r(\lambda). \quad (3.29)$$

Combining (3.28) and (3.29), ${}^\phi S_{ijkm}$ becomes

$${}^\phi S_{ijkm} = \sum_{r=1}^{N_\Lambda} {}^\phi k_r(ijkm) \chi_r(\lambda) + \sum_{l=0}^4 \sum_{m=-l}^{+l} \sum_{n=-l}^{+l} \sum_{r=1}^{N_\Lambda} {}^\phi \alpha_r {}^\phi D_l^{*mn}(ijkm) T_l^{*mn}(g) \chi_r(\lambda). \quad (3.30)$$

The stiffness lower bound, before inversion, is found by joining equations (2.15), (3.21), and (3.30),

$$\langle S_{ijkl} \rangle = \sum_{\phi=1}^n \sum_{l=0}^4 \sum_{m=-l}^{+l} \sum_{n=-l}^{+l} \sum_{r=1}^{N_\Lambda} [\phi k_r(ijkm) \delta_{l0} + \phi \alpha_r \phi D_l^{*mn}(ijkm)] \phi F_{lr}^{mn}. \quad (3.31)$$

3.4.1 Inversion of the Lower Bound

By setting $\sigma_{ij} = \sigma_{ji}$ and $\varepsilon_{ij} = \varepsilon_{ji}$ the fourth rank tensor reduces from 81 terms to 36 terms, which can be written in matrix form as

$$\begin{bmatrix} \varepsilon_{11} \\ \varepsilon_{22} \\ \varepsilon_{33} \\ \varepsilon_{23} \\ \varepsilon_{31} \\ \varepsilon_{12} \\ \varepsilon_{23} \\ \varepsilon_{31} \\ \varepsilon_{12} \end{bmatrix} = \begin{bmatrix} S_{1111} & S_{1122} & S_{1133} & S_{1123} & S_{1131} & S_{1112} & S_{1123} & S_{1131} & S_{1112} \\ S_{1122} & S_{2222} & S_{2233} & S_{2223} & S_{2231} & S_{2212} & S_{2223} & S_{2231} & S_{2212} \\ S_{1133} & S_{2233} & S_{3333} & S_{3323} & S_{3331} & S_{3312} & S_{3323} & S_{3331} & S_{3312} \\ S_{1123} & S_{2223} & S_{3323} & S_{2323} & S_{2331} & S_{2312} & S_{2323} & S_{2331} & S_{2312} \\ S_{1131} & S_{2231} & S_{3331} & S_{2331} & S_{3131} & S_{3112} & S_{2331} & S_{3131} & S_{3112} \\ S_{1112} & S_{2212} & S_{3312} & S_{2312} & S_{3112} & S_{1212} & S_{2312} & S_{3112} & S_{1212} \\ S_{1123} & S_{2223} & S_{3323} & S_{2323} & S_{2331} & S_{2312} & S_{2323} & S_{2331} & S_{2312} \\ S_{1131} & S_{2231} & S_{3331} & S_{2331} & S_{3131} & S_{3112} & S_{2331} & S_{3131} & S_{3112} \\ S_{1112} & S_{2212} & S_{3312} & S_{2312} & S_{3112} & S_{1212} & S_{2312} & S_{3112} & S_{1212} \end{bmatrix} \begin{bmatrix} \sigma_{11} \\ \sigma_{22} \\ \sigma_{33} \\ \sigma_{23} \\ \sigma_{31} \\ \sigma_{12} \\ \sigma_{23} \\ \sigma_{31} \\ \sigma_{12} \end{bmatrix}. \quad (3.32)$$

(3.32) is furthered reduced by applying crystal symmetry. Since the determinant of a fourth-order tensor is typically zero, equation (3.32) is reduced by symmetry to a six-by-six tensor (Hirth and Lothe 1968). One shortcoming of the six-by-six tensor is that rotations can only be performed on the fourth rank tensor. Using a two index method, Table 3.1, the fourth-order tensor reduces to, S_{ij}

Table 3.1 Transforming from four indices, S_{ijkl} , to two indices, S_{ij}

Four Indices	11	22	33	23	31	12
Two Indices	1	2	3	4	5	6

$$\begin{bmatrix} S_{11} & S_{12} & S_{13} & S_{14} & S_{15} & S_{16} \\ S_{12} & S_{22} & S_{23} & S_{24} & S_{25} & S_{26} \\ S_{13} & S_{23} & S_{33} & S_{34} & S_{35} & S_{26} \\ S_{14} & S_{24} & S_{34} & S_{44} & S_{45} & S_{46} \\ S_{15} & S_{25} & S_{35} & S_{45} & S_{55} & S_{56} \\ S_{16} & S_{26} & S_{26} & S_{46} & S_{56} & S_{66} \end{bmatrix}. \quad (3.33)$$

This six-by-six tensor is then inverted forming a new six-by-six primed tensor⁴, S'_{ij} ,

$$\begin{bmatrix} S'_{11} & S'_{12} & S'_{13} & S'_{14} & S'_{15} & S'_{16} \\ S'_{12} & S'_{22} & S'_{23} & S'_{24} & S'_{25} & S'_{26} \\ S'_{13} & S'_{23} & S'_{33} & S'_{34} & S'_{35} & S'_{26} \\ S'_{14} & S'_{24} & S'_{34} & S'_{44} & S'_{45} & S'_{46} \\ S'_{15} & S'_{25} & S'_{35} & S'_{45} & S'_{55} & S'_{56} \\ S'_{16} & S'_{26} & S'_{26} & S'_{46} & S'_{56} & S'_{66} \end{bmatrix}. \quad (3.34)$$

This new prime tensor is transformed back to the unprimed state by

$$\begin{aligned} S_{ij} &= S'_{ij} \quad \text{where } i \text{ and } j \leq 3 \\ S_{ij} &= \frac{1}{2} S'_{ij} \quad \text{where either } i \text{ or } j \text{ is } 4, 5, 6. \\ S_{ij} &= \frac{1}{4} S'_{ij} \quad \text{where both } i \text{ and } j \text{ is } 4, 5, 6 \end{aligned} \quad (3.35)$$

⁴ There is some disagreement in the literature on which tensor should be primed, this work choose to use the same terminology as Hirth and Lothe (1968).

After the prime tensor has been transformed into the unprimed state, it is a simple matter to unfold the six-by-six tensor back into the fourth rank tensor. From the fourth rank tensor the correct $\langle S \rangle_{ijkm}^{-1}$ is extracted.

4 Alloy System

4.1 Overview

The elastic bounds are dependent on material constants, i.e. ${}^\phi C_{ij}^\circ(\lambda)$ and ${}^\phi S_{ij}^\circ(\lambda)$.

The isomorphous FCC alloy of copper and nickel was chosen for analysis, to demonstrate how symmetry enters into the equations of Chapter 3. The phase diagram for the Cu-Ni system is shown in Figure 4.1 (Massalski, 1986). Hartley's study of this system at room temperature reported negligible discontinuity in slope of the elastic constants at compositions where the ordered α_1 and α_2 phases make their appearance (see Figure 3.5).

4.2 Elastic Bounds with Crystal and Sample Symmetry

The crystal symmetry of the Cu-Ni system is cubic. Additionally, orthorhombic sample symmetry is introduced. Orthorhombic sample symmetry occurs for thin sheets where out of plane stress and strain can be ignored. It consists of three mutually-perpendicular 2-fold rotations, associated with the principal directions of the processing (usually rolling) (Knocks *et. al.* 1998). From these symmetries, equation (3.21) is reduced from 36 elements to 9 independent elements, represented by a six-by-six tensor of the form:

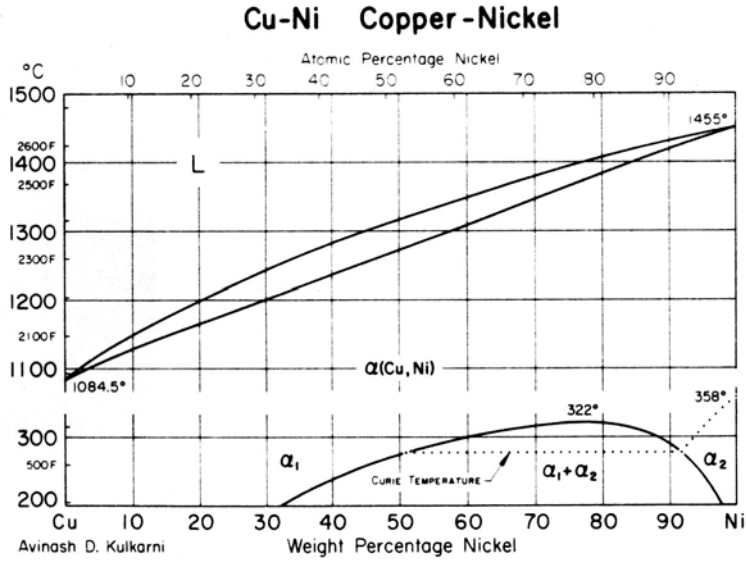


Figure 4.1 Copper-Nickel alloy system

$$\begin{bmatrix} S_{11} & S_{12} & S_{13} & - & - & - \\ S_{12} & S_{22} & S_{23} & - & - & - \\ S_{13} & S_{23} & S_{33} & - & - & - \\ - & - & - & S_{44} & - & - \\ - & - & - & - & S_{55} & - \\ - & - & - & - & - & S_{66} \end{bmatrix}. \quad (4.1)$$

Upon consideration of the cubic-orthorhombic symmetry, the Fourier basis functions change to ${}^\phi\dot{\tilde{T}}_l^{\mu\eta}(g)$ (Bunge 1982), where the dots indicate that symmetry has been imposed, as described in equation (2.6). The piecewise constant functions do not change with symmetry. For the following equations the $T_l^{mn}(g)$ functions are transformed into ${}^\phi\dot{\tilde{T}}_l^{\mu\eta}(g)$. The description of the Dirac functions, equation (2.11), becomes

$$\delta(h - h_j) = \sum_{\phi=1}^1 \sum_{l=0}^{\infty} \sum_{\mu=1}^{\phi M(l)} \sum_{\nu=1}^{\phi N(l)} \sum_{r=1}^{N_\Lambda} {}^\phi\dot{\tilde{F}}_{lr}^{\mu\nu} {}^\phi\dot{\tilde{T}}_l^{\mu\nu}(g_j) \chi_r(\lambda_j), \quad (4.2)$$

where ${}^\phi\dot{\tilde{F}}_{lr}^{\mu\nu}$, are described as

$${}^{\phi}\dot{\tilde{F}}_{lr}^{\mu\nu} = (2l+1)M(\lambda_j) {}^{\phi}\dot{\tilde{T}}_l^{*\mu\nu}(g_j) \chi_r(\lambda_j). \quad (4.3)$$

Here ${}^{\phi}M(l)$ enumerates the crystal symmetric subspaces associated with the phase ϕ and the index l , and ${}^{\phi}N(l)$ enumerates the sample symmetric subspaces (Bunge (1982), as tabulated in Figures 4.2 and 4.3

When symmetry is considered, the local state distribution function, (2.15), becomes

$$f(\phi, g, \lambda) = \sum_{l=0}^{\infty} \sum_{\mu=1}^{\phi M(l)} \sum_{\nu=1}^{\phi N(l)} \sum_{r=1}^{N_\Lambda} {}^{\phi}\dot{\tilde{F}}_{lr}^{\mu\nu} {}^{\phi}\dot{\tilde{T}}_l^{\mu\nu}(g) \chi_r(\lambda). \quad (4.4)$$

(3.16) changes to

$${}^{\phi}Z_{ijkm} = \sum_{l=0,4}^4 \sum_{\nu=1}^{\phi N(l)} \sum_{r=1}^{N_r} {}^{\phi}\beta_r {}^{\phi}\dot{\tilde{D}}_l^{*1\nu}(ijkm) {}^{\phi}\dot{\tilde{T}}_l^{*1\nu}(g) \chi_r(\lambda), \quad (4.5)$$

and (3.17) transforms into

$$g_{ri}g_{rj}g_{rk}g_{rm} = \sum_{l'=0,4}^4 \sum_{\nu'=1}^{\phi N(l)} {}^{\phi}\dot{\tilde{D}}_{l'}^{1\nu'}(ijkm) {}^{\phi}\dot{\tilde{T}}_{l'}^{1\nu'}(g). \quad (4.6)$$

Equation (3.18) becomes

$${}^{\phi}C_{ijkm} = \sum_{r=1}^{N_\Lambda} {}^{\phi}k_r(ijkm) \chi_r(\lambda) + \sum_{l=0,4}^4 \sum_{\nu=1}^{\phi N(l)} \sum_{r=1}^{N_\Lambda} {}^{\phi}\beta_r {}^{\phi}\dot{\tilde{D}}_l^{*1\nu}(ijkm) {}^{\phi}\dot{\tilde{T}}_l^{*1\nu}(g) \chi_r(\lambda). \quad (4.7)$$

Looking at the lower bound, (3.29) becomes

$${}^{\phi}Q_{ijkm} = \sum_{l=0,4}^4 \sum_{\nu=1}^{\phi N(l)} \sum_{r=1}^{N_\Lambda} {}^{\phi}\alpha_r {}^{\phi}\dot{\tilde{D}}_l^{*1\nu}(ijkm) {}^{\phi}\dot{\tilde{T}}_l^{*1\nu}(g) \chi_r(\lambda), \quad (4.8)$$

and (3.30) is

$${}^{\phi}S_{ijkm} = \sum_{r=1}^{N_\Lambda} {}^{\phi}k_r(ijkm) \chi_r(\lambda) + \sum_{l=0,4}^4 \sum_{\nu=1}^{\phi N(l)} \sum_{r=1}^{N_\Lambda} {}^{\phi}\alpha_r {}^{\phi}\dot{\tilde{D}}_l^{*1\nu}(ijkm) {}^{\phi}\dot{\tilde{T}}_l^{*1\nu}(g) \chi_r(\lambda). \quad (4.9)$$

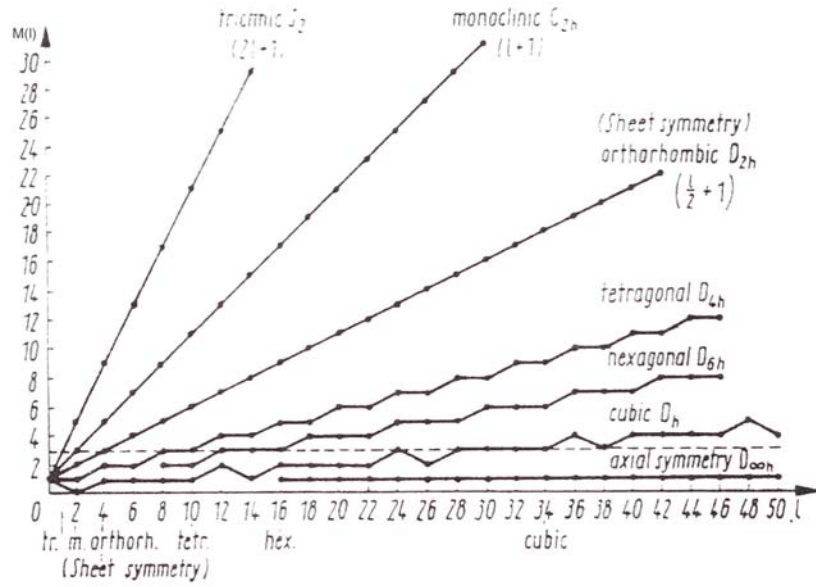


*Figure 4.2 Number of linearly independent spherical harmonics of different symmetries as a function of degree l (for even l).
(Bunge 1982)*

Finally equations (3.19) and (3.31) carry the cubic-orthorhombic symmetry, and for two-phase examples these become

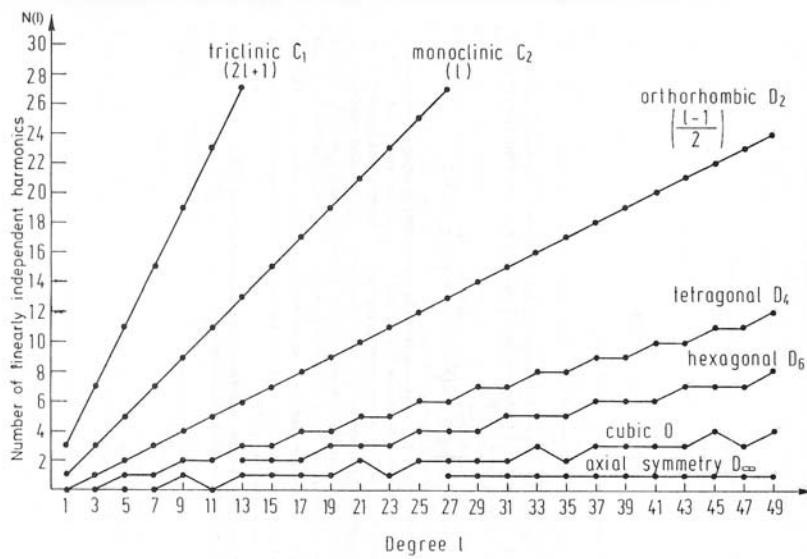


Figure 4.3 Number of linearly independent spherical harmonics of different symmetries as a function of degree l (for odd l). (Bunge 1982)

$$C_{ijkm}^* \leq \langle C_{ijkm} \rangle = \sum_{\phi=1}^1 \sum_{l=0,4}^4 \sum_{\mu=1}^{\phi N(l)} \sum_{r=1}^{N_\Lambda} [\phi k_r(ijkm) \delta_{l0} + \phi \beta_r \phi \dot{D}_l^{*1\mu}(ijkm)] \phi \dot{F}_{lr}^{1\mu}, \quad (4.10)$$

$$C_{ijkm}^* \geq \langle S \rangle_{ijkm}^{-1} = \left[\sum_{\phi=1}^1 \sum_{l=0}^4 \sum_{\mu=1}^{\phi N(l)} \sum_{r=1}^{N_\Lambda} [\phi k_r(pqst) \delta_{l0} + \phi \alpha_r \phi \dot{D}_l^{*1\mu}(pqst)] \phi \dot{F}_{lr}^{1\mu} \right]^{-1}. \quad (4.11)$$

However, as the case study consists of a single phase the sum over ϕ is omitted. Appendix B shows an explicit inversion for the single-phase cubic-orthorhombic case of (4.11).

5 Elastic Properties in Fourier Space

5.1 Overview

The elastic bounds are expressed as a hyper-plane (4.10) for the upper-bound, and a hyper-surface (4.11) for the lower-bound on C_{ijkm}^* , within the common spectral language. These hyper-surfaces translate through the microstructure hull depending on the selected property value of C_{ijkm}^* . From these translations the extreme property limits are computed. Additionally these hyper-surfaces are used to identify pockets of microstructures that fulfill the design objectives.

5.2 Hyper-Surfaces in the Fourier Space

Chapter 2 introduced the microstructure hull which represents all possible microstructures, expressed by equation (2.16). Points outside the microstructure hull are fictitious microstructures, having no physical meaning. The hyper-surfaces therefore only have meaning within the microstructure hull.

A graphical depiction of (4.10) shows that the elastic upper-bound forms hyper-planes in the multidimensional Fourier space, as shown in Figure 5.1. These hyper-planes have a set property-bound value for all points that lie upon the plane, i.e. in Figure 5.1 the $\langle C_{1111} \rangle$ plane has a value of 200 GPa. As the hyper-planes are translated through the spectral representation, property extremes are observed. These extremes are used to

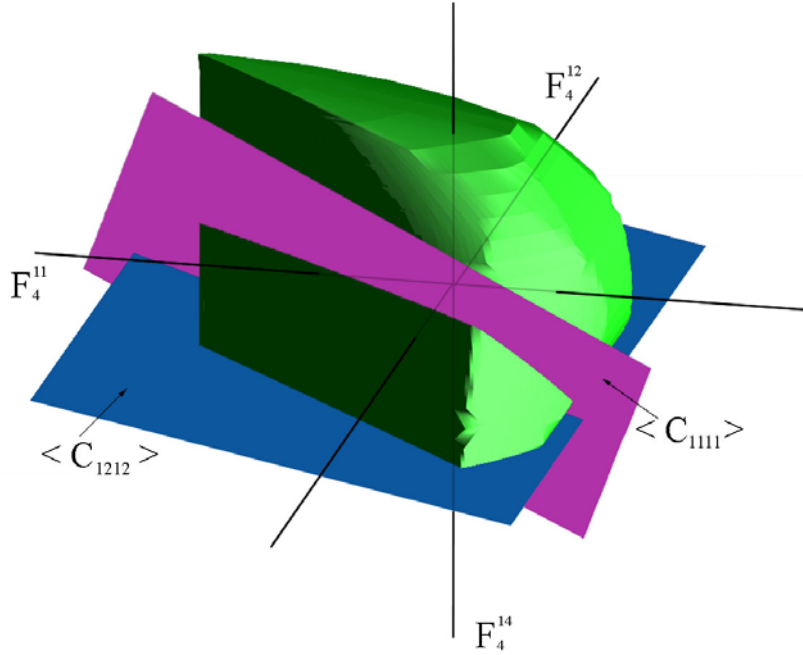


Figure 5.1 Elastic upper-bound of $\langle C_{1111} \rangle$ and $\langle C_{1212} \rangle$ in the microstructure hull

identify the property closures introduced in Chapter 6. Figure 5.1 shows that each plane traverses through the microstructure hull with different plane normals. These plane normals are listed in Table 5.1 for the cubic-orthorhombic case.

Some characteristic of the hyper-planes are that the $\langle C_{1111} \rangle$ hyper-plane yields higher stiffness values as the plane moves negatively along the F_4^{12} axis. $\langle C_{1212} \rangle$ yields higher stiffness values as the plane translates positively along the F_4^{14} axis. Appendix D contains computer code for calculating points on a set hyper-plane.

Table 5.1 $D_l^{1\mu}$ coefficients for the cubic-orthorhombic case for the on-diagonal elements

$ijkm$	$l=0;\mu=1$	$l=4;\mu=1$	$l=4;\mu=2$	$l=4;\mu=4$
1111	0.599939	0.195980	-0.292770	0.387240
2222	0.599939	0.195980	0.292770	0.387240
3333	0.599919	0.523168	0	0
2323	0.200000	-0.261861	-0.292770	0
3131	0.200000	-0.261861	0.292770	0
1212	0.199980	0.065327	0	-0.387240

Equation (4.11) produces a hyper-surface for the elastic lower-bound. Figure 5.2 shows the $\langle S \rangle_{1111}^{-1}$ hyper-surface within the microstructure hull (Note: the axes have changed from Figure 5.2 to show the curvature of the hyper-surface). Not all of the lower-bounds are hyper-surfaces for the cubic-orthorhombic elastic stiffness case. Only the $\langle S \rangle_{iii}^{-1}$ terms (no sum on i) are hyper-surfaces. The $\langle S \rangle_{ijj}^{-1}$ terms (no sum on i or j) are only a simple inverse and do not produce the complicated terms as seen with $\langle S \rangle_{iii}^{-1}$. For an explicit description of the inverse for the lower-bound see appendix H.

Again the $\langle S \rangle_{1111}^{-1}$ hyper-surface yields larger property values if the hyper-surface is translated along the negative F_4^{12} axis. Additional hyper-surfaces can be found for other lower-bounds and the general characteristics are the same as the upper-bound hyper-plane. Appendix E contains computer code for calculating points for a set hyper-surface.

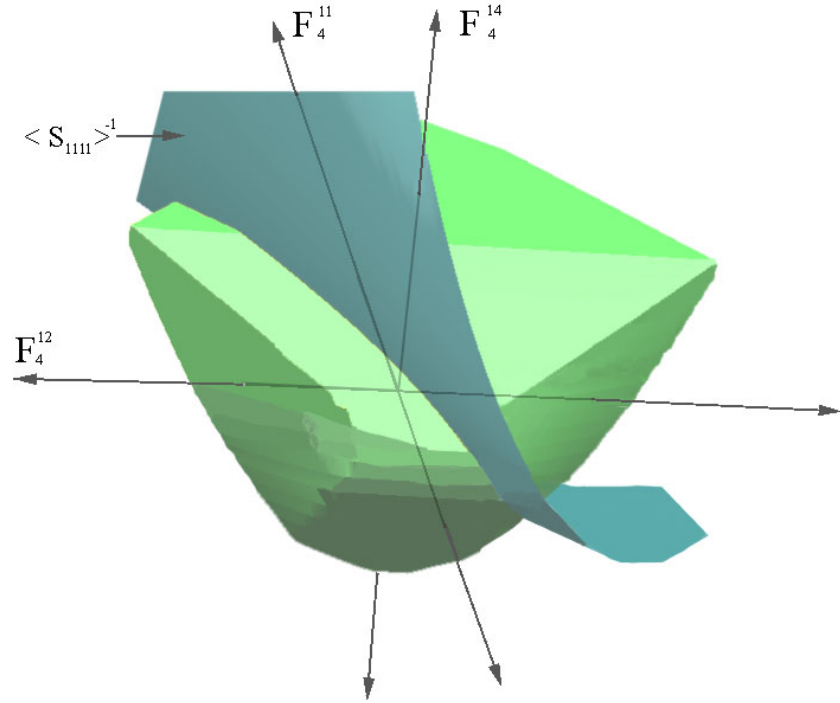


Figure 5.2 Elastic lower-bound of the hyper-surface $< S >_{1111}^{-1}$ in the microstructure hull

As these hyper-surfaces are added to the microstructure hull, they are used to find groups of microstructures that fulfill the design objectives. As more design properties are included, it becomes more difficult to find microstructures that fulfill all design constraints. Looking at two properties such as C_{1111}^* and C_{1212}^* , an area of the microstructure hull is found that satisfies both constraints and is represented as the area in yellow on Figure 5.3. For C_{1111}^* the lower bound $< S >_{1111}^*$ is used, and for C_{1212}^* the upper bound is expressed. This area contains multiple microstructures that satisfy the design constraints chosen by the design engineer..

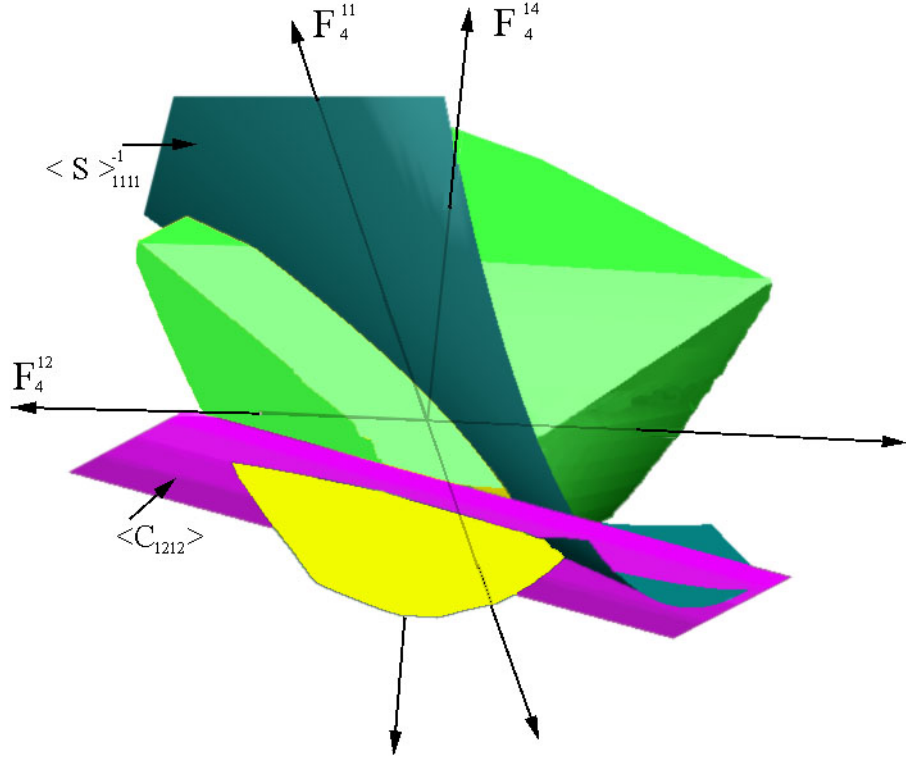


Figure 5.3 Microstructure hull with $< S >_{1111}^{-1}$ and $< C_{1212} >$ hyper-surfaces. The area in yellow contains those microstructures that fulfill the design constraints.

5.3 Extraction of Microstructures from the Fourier Space

Once an area has been identified that satisfies the design criteria the next step is to extract microstructures. The purpose of this thesis was not on the extraction process, but a brief overview is included to demonstrate the next step in the MSD method. The microstructures are extracted by first finding the boundaries of the desired area. By locating these boundaries, sets of F_{lr}^{1v} coefficients are known. From equation (2.15) these F_{lr}^{1v} coefficients are used to find sets of local state distributions, $f(h)$. These local state distribution functions detail the sets of microstructures that satisfy the design objectives.

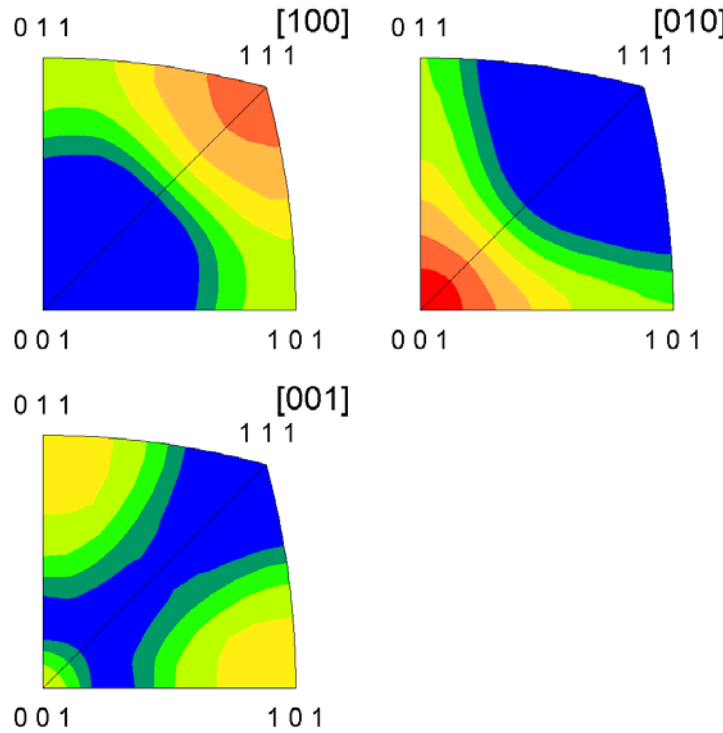


Figure 5.4 One extracted microstructure that satisfy both the $\langle S \rangle_{1111}^{-1}$ and $\langle C_{1212} \rangle$ bounds.

Figure 5.4 shows one microstructure extracted from the yellow area in Figure 5.3. The constraints associated with the yellow region in Figure 5.3 are described in section 6.3.

6 Property Closures

6.1 Overview

Property closures are generated by condensing the information contained within the multi-dimensional Fourier space into representations of lower-dimensionality (e.g., 2-D). This compaction of information is beneficial for a quick determination of combined property limits for a particular alloy system. The property closures are determined by taking two (or more) property hyper-surfaces found in Chapter 4 through the entire microstructure hull. From this analysis a closure is formed that encompasses all possible values for the combined properties. The property closures contain only partial information from the microstructure hull. The property closures can be used to identify if there are any microstructures that fulfill the design criteria, but individual microstructures can only be extracted from the microstructure hull.

6.2 Generation of the Property Closures

For computation of property closures, two properties are selected. These could be elastic properties or any other property expressed with Fourier coefficients. Only the upper bound, (4.10), is required for computation of an elastic property closure since the bounds on elastic properties coincide for single crystalline microstructures, and these

occur at the periphery of the microstructure hull, and also at the periphery of the properties closures.

One approach to generating a 2-D property closure was: one property, i.e. C_{1111}^* , is kept constant while the other property, i.e. C_{1212}^* , is allowed to move through the microstructure hull. Since the microstructure hull is calculated from discrete points there are no formulas for the boundaries. Due to this limitation of the microstructure hull, another approach was used for generating property closures. The cubic-orthorhombic orientation space was divided into equal volume boxes. These boxes were then used to calculate the properties over all orientations, including multiple orientations. From these calculations the extremes were found by keeping one property constant, i.e. C_{1111}^* , and find the min and max of the second property, i.e. C_{1212}^* . These extremes form the outer region of the property closure. Various algorithms can be used since finding the property closures is simply a min/max problem (Belegundu and Chandrupatla, 1999). For calculating many property closures, or higher-dimensional closures, a faster algorithm would be required. Figure 6.1 shows how these extremes are viewed in a 2-D representation.

6.3 Benefits of the Property Closures

The property closures, used in conjunction with the microstructure hull and the hyper-surface construction, can identify alloy microstructures that fulfill the selected design objectives. The design criteria dictates the minimum property values that fulfill the design objective. These criteria are used to set the effective properties, e.g property C_{1111}^* and C_{1212}^* . For example, if C_{1111}^* must be greater than 320 GPa, illustrated

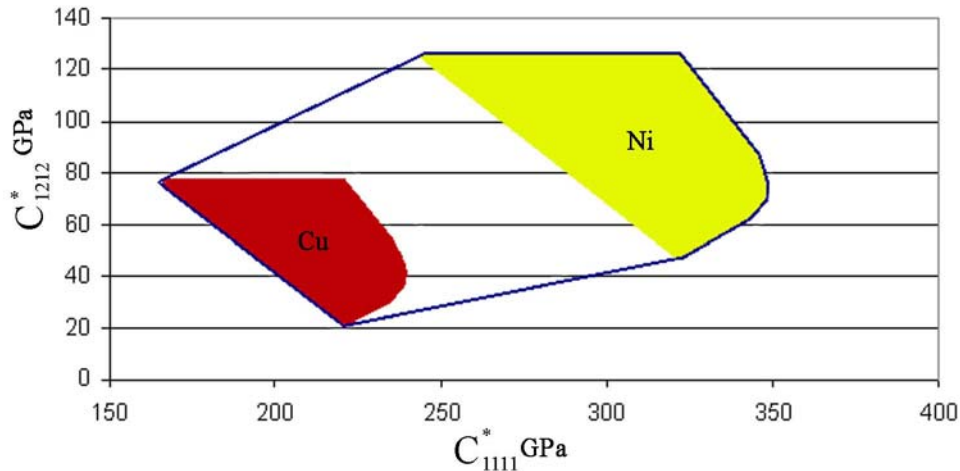


Figure 6.1 Property closure of C_{1111}^* vs. C_{1212}^* of the Cu-Ni alloy system

by A in Figure 6.2, C_{1212}^* must be less than 63 GPa, illustrated by B . From Figure 6.2 there is a small area of microstructures that can fulfill both property objectives. Therefore, it is known that for these two effective properties, sets of microstructures exist that solve the design objectives. Additional property closures, for the on-diagonal elements, can be found in Appendix A.

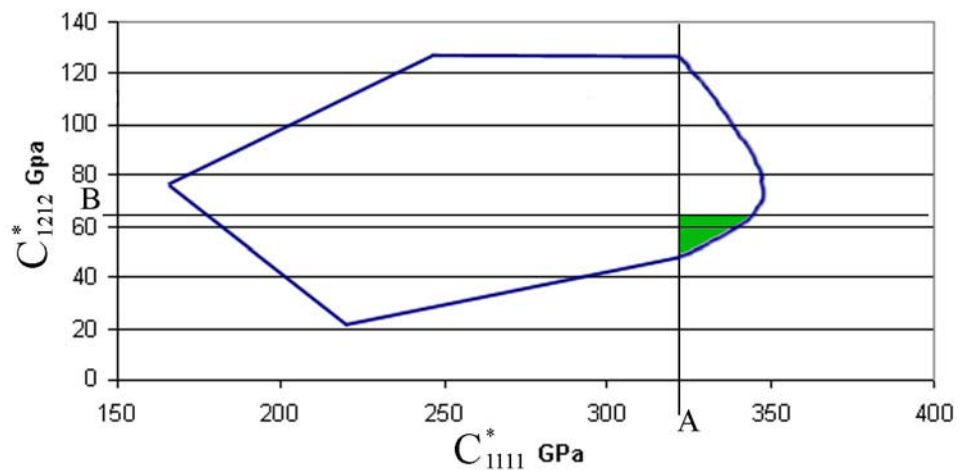


Figure 6.2 Property closure of C_{1111}^* vs. C_{1212}^* with design constraints added at A and B

7 Conclusions and Recommendations

7.1 Conclusions

Through the use of MSD a method of communication between the Design Engineer, Material Scientist, and Materials Manufacturing Specialist (Processor) has been developed. This common language allows the design criteria to dictate what properties are improved, instead of the Material Scientist and Processor guessing what properties will be of importance. The Fourier space yields sets of solutions that can include both single and polycrystalline materials. These polycrystalline solutions yield less expensive solutions compared to single crystal solutions.

The property closures contain only partial information from the microstructure hull. The property closures can be used to identify if there are any microstructures that fulfill the design criteria, but individual microstructures can only be extracted from the microstructure hull. Through this combination of MSD tools difficult design problems may be solved for multiple design constraints.

The process of transforming properties into the spectral representation is mathematically intensive, but once this process has been achieved the properties can be employed to solve a multitude of design problems. For design problems of equal local state variables, the spectral representation remains the same.

7.2 Recommendations

The Hill bounds were used to find the effective stiffness tensor; for the Hill bounds the variance from actual results is large compared to the elastic bounds recovered from two-point statistics (Mason, 1999). Hill bounds may be used for design work, but there is a significant spread of results from the upper and lower bounds. By using the two-point statistics this spread is greatly reduced and more accurate results can be achieved. The two-point statistics are realized through Green's functions. These Green's functions increase the degree of difficulty in transforming the bounds, but the additional accuracy may be sufficient to warrant the effort.

The off diagonal elements of the effective stiffness tensor are required in some design problems. It is known that these elements have a coupling with the diagonal elements (Cherkaev, 2000). A better understanding of this coupling and how to recover the off diagonal elements is of importance.

As design problems leave the simple case of cubic-orthorhombic symmetry the dimensionality of the Fourier space increases dramatically. Therefore optimization routines are required for solving multiple design criteria in 10, 50, or an even larger number of Fourier dimensions.

References

- Adams, B. L., Henrie, A., Henrie, B., Lyon, M., Kalidindi, S. R., Garmestani, H. (2001) Microstructure-Sensitive Design of a Compliant Beam, *Journal of Mechanics and Physics of Solids*, 49:1639-1663.
- Adams, B. L., Olsen T. (1998) The mesostructure-properties linkage in polycrystals, *Progress in Material Science*, 43:1-88.
- Ashby, M. F. (1992) *Materials Selection in Mechanical Design*, Pergamon Press Inc., New York.
- Belegundu, A. D., Chandrupatla, T. R. (1999), *Optimization Concepts and Applications in Engineering*, Prentice-Hall, Inc, New Jersey.
- Beran, M. J., Mason, T. A., Adams, B. L., and Olson, T. (1996) Bounding elastic constants of an orthotropic polycrystal from measurements of the microstructure, *Journal of Mechanics and Physics of Solids*, 44:1543-63.
- Bunge, H. J. (1982) *Texture Analysis in Materials Science*, Butterworths, London.
- Cherkaev, A. (2000) *Variational Methods for structural optimization*, Springer, New York.
- Courant, R., and Hilbert, D. (1989) *Methods of Mathematical Physics*, Wiley-Interscience, New York.
- Hartley, C. S. (2001) *Single Crystal Elastic Module of Disordered Cubic Alloys Part I: Face-Centered Cubic Systems*, Submitted for publication.
- Hashin, Z., and Shtrikman, S. (1962a) On some Variational Principles in Anisotropic and Nonhomogeneous Elasticity, *J. Mech. Phys. Solids*, 10: 335-342.

- Hashin, Z., and Shtrikman, S. (1962b) A Variational Approach to the Theory of the Elastic Behavior of Polycrystals, *J. Mech. Phys. Solids*, 10: 343-352.
- Hill, R. (1952) The Elastic Behavior of a Crystalline Aggregate, *Proc. Phys. Soc. Lond.*, A 65: 349-354.
- Hirth, J. P. and Lothe, J. (1968) *Theory of Dislocations*, McGraw-Hill, Inc.
- Howell, L.L., (2001) *Compliant Mechanisms*, Wiley-Interscience.
- Keener, J. P., (2000) *Principles of Applied Mathematics*, 2nd Ed., Perseus, Cambridge, Mass.
- Knocks, U. F., Tome, C. N., and Wenk H.-R. (1998) *Texture and Anisotropy*, Cambridge University Press.
- Larsen, U. D., Sigmund, O., and Bouwstra, S. (1997) Design and Fabrication of Compliant Micromechanisms and Structures with Negative Poisson's Ratio, *Journal of Microelectromechanical Systems*, Vol 6, No 2: 99-106.
- Mason, T. A., and Adams, B. L., (1999) Use of Microstructural Statistics in Predicting Polycrystalline Material Properties, *Meturgical and Materials Transaction A*, 30A:969-79.
- Massalski, T. B. (1986), *Binary Alloy Phase Diagrams*, American Society for Metals.
- Olhoff, N., Ronholt, E., and Scheel, J. (1998) Topology Optimization of Three-Dimensional Structures using Optimum Microstructures, *Structural Optimization*, 16: 1-18.
- Olsen, G. B. (1998) System design of hierarchically structured materials: Advanced steels, *Journal of computer-aided materials design*, Vol 4, issue 3 143-156.
- Reuss, A. (1929) *Z. Angew. Math. Mech.*, 9: 49-58.
- Sigmund, O., Torquato, S., and Aksay, I. A. (1998) On the Design of 1-3 Piezocomposites using Topology Optimization, *J. Mater. Res.* 13: 1038-1048.
- Strayer, J. K. (1989) *Linear Programming and Its Applications*, Springer-Verlag New York Inc.

Subbarayan, G., and Raj, R. (1999) A Methodology for Integrating Materials Science with System Engineering, *Materials and Design*, 20: 1-12.

Voigt, W. (1928) *Lehrbuch der Kristallphysik*, Teubner, Leipzig.

Appendix

Appendix A : Property Closures

The following property closures are for the Cu-Ni alloy system.

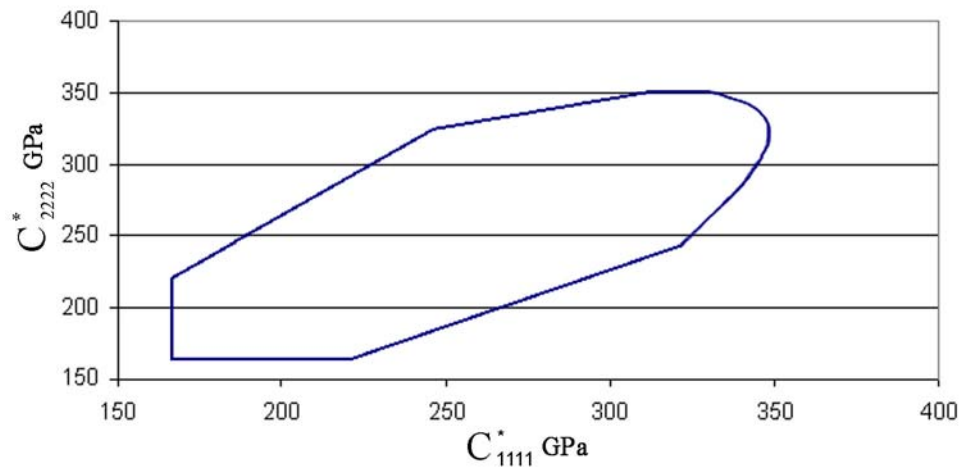


Figure A.1 Property closure of C^*_{1111} vs. C^*_{2222}

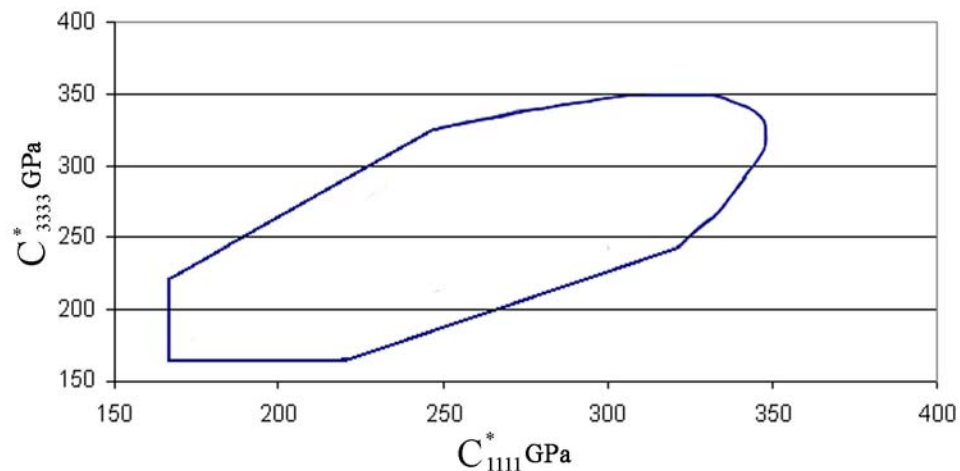


Figure A.2 Property closure of C^*_{1111} vs. C^*_{3333}

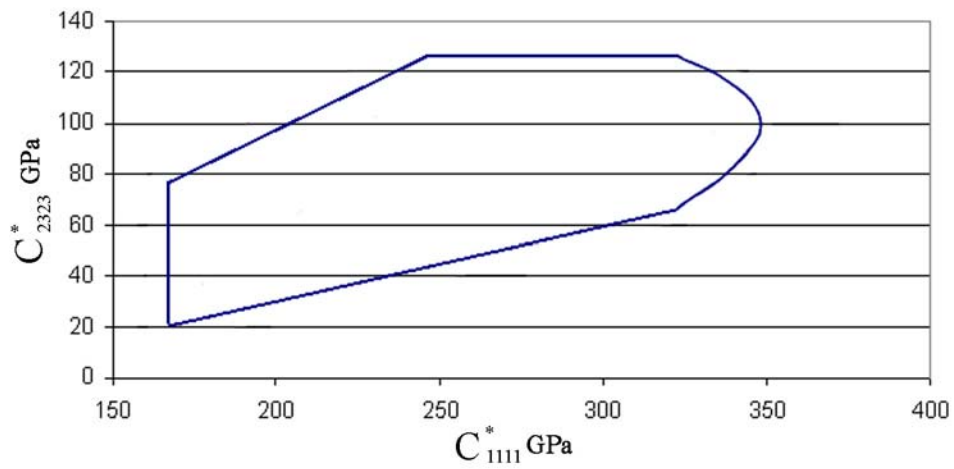


Figure A.3 Property closure of C_{1111}^ vs. C_{2323}^**

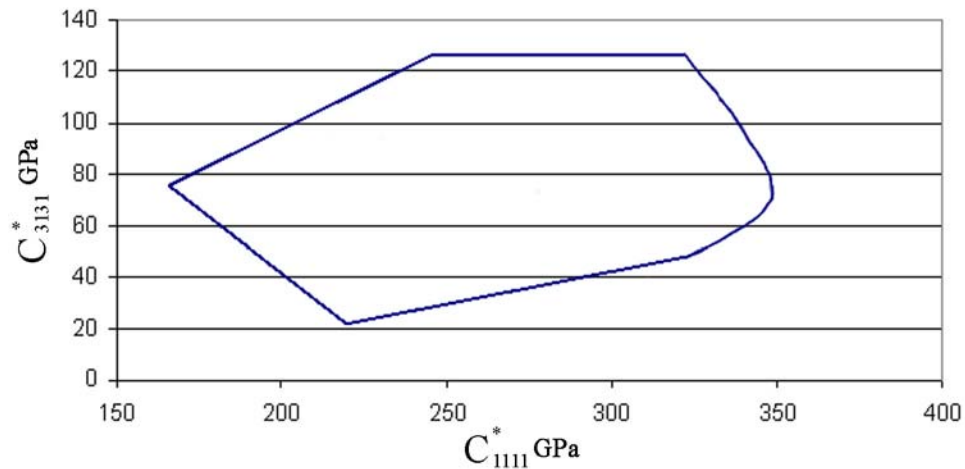


Figure A.4 Property closure of C_{1111}^ vs. C_{3131}^**

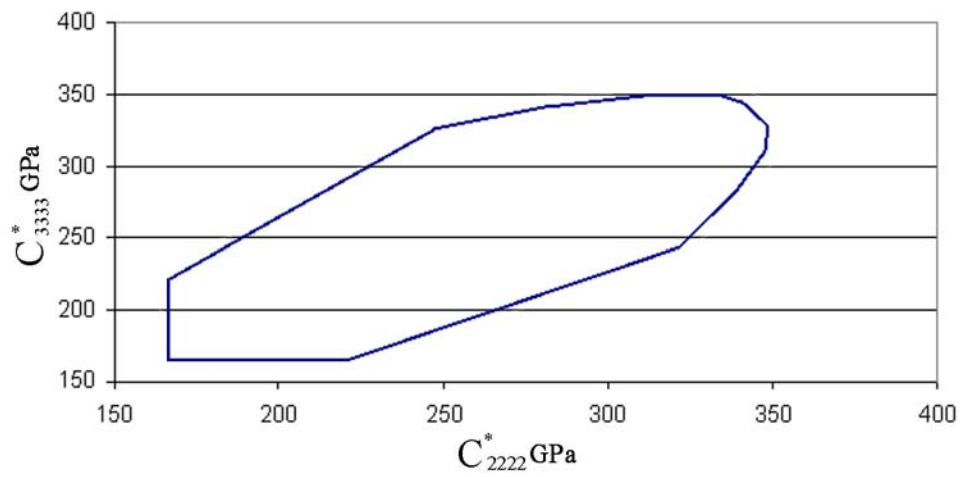


Figure A.5 Property closure of C^*_{2222} vs. C^*_{3333}

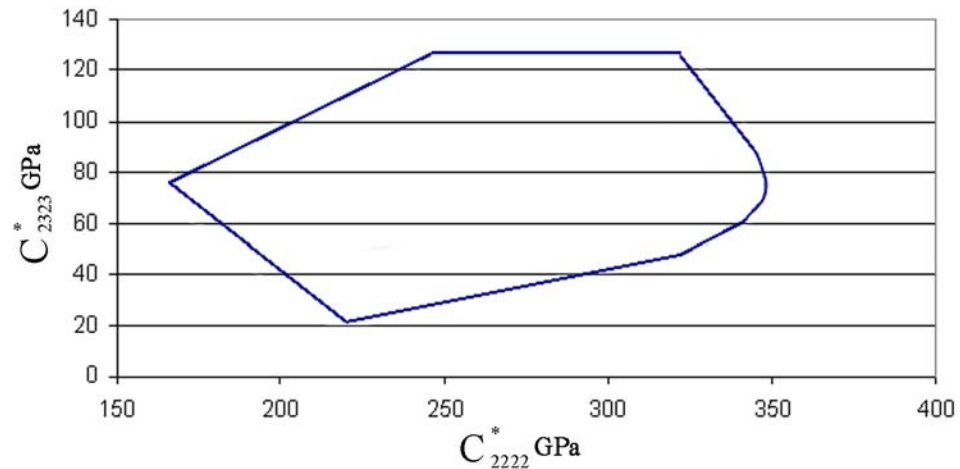


Figure A.6 Property closure of C^*_{2222} vs. C^*_{2323}

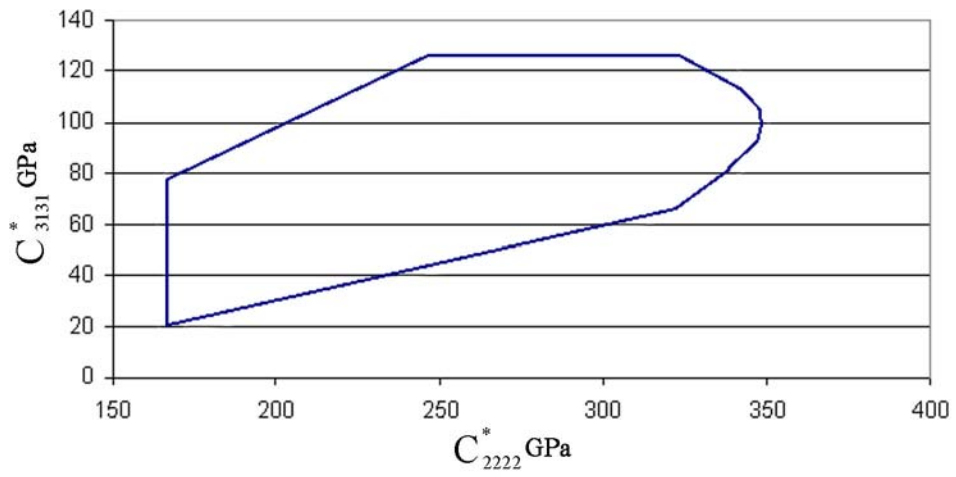


Figure A.7 Property closure of C_{2222}^* vs. C_{3131}^*

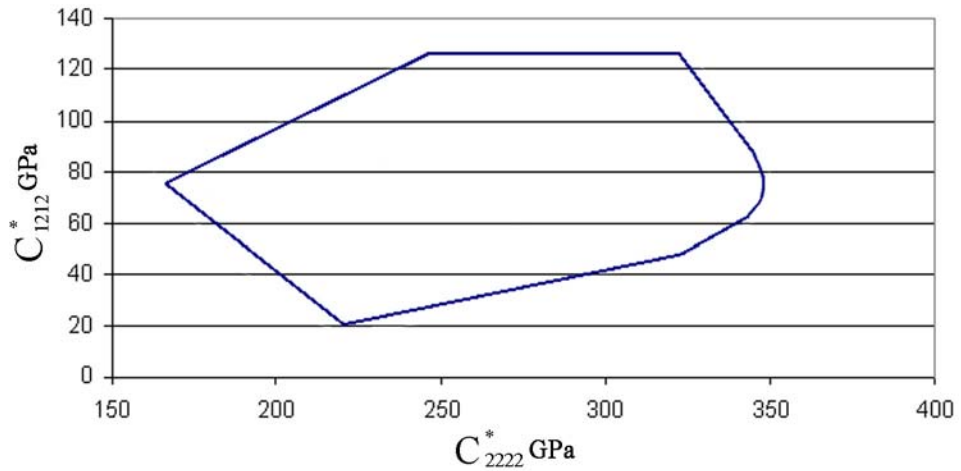


Figure A.8 Property closure of C_{2222}^* vs. C_{1212}^*

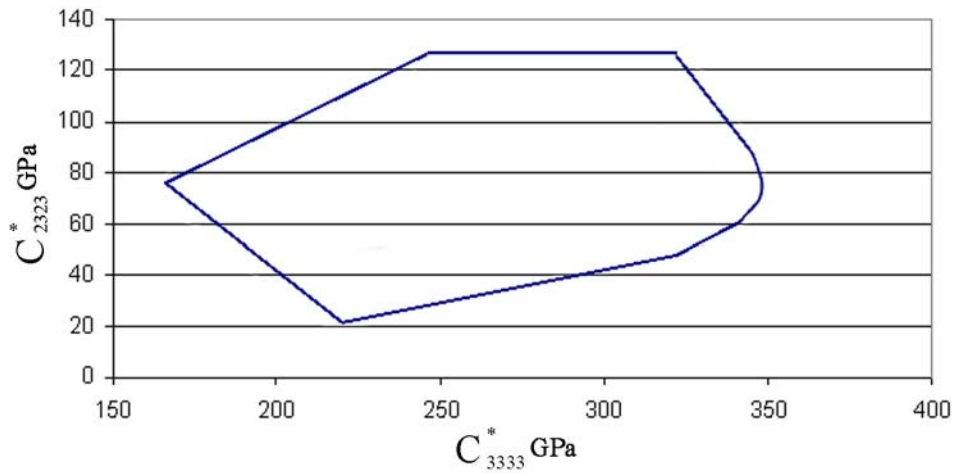


Figure A.9 Property closure of C_{3333}^* vs. C_{2323}^*

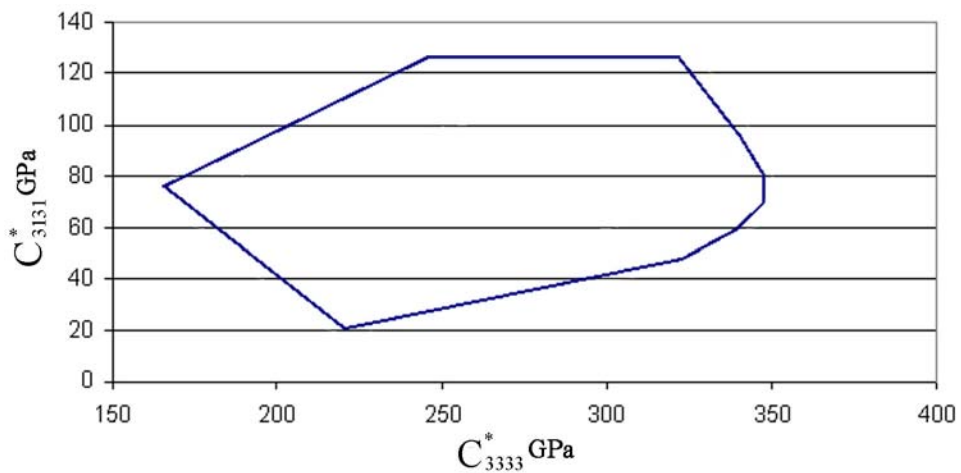


Figure A.10 Property closure of C_{3333}^* vs. C_{3131}^*

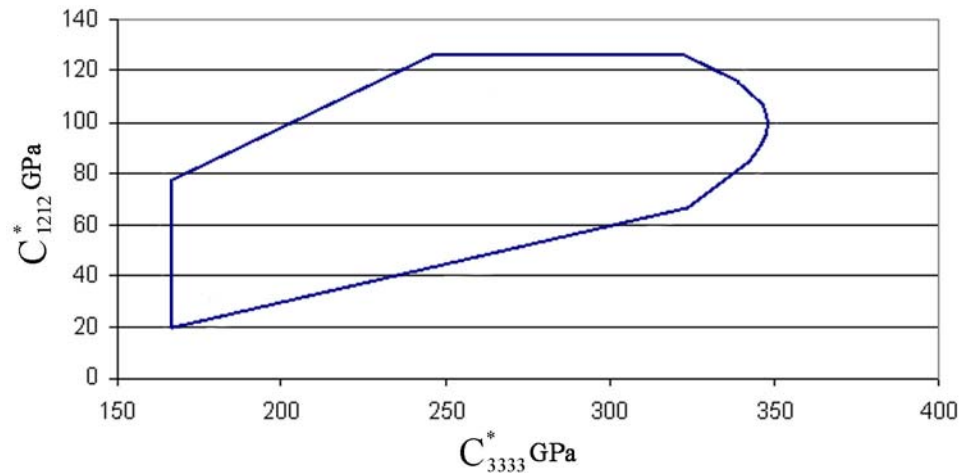


Figure A.11 Property closure of C_{3333}^* vs. C_{1212}^*

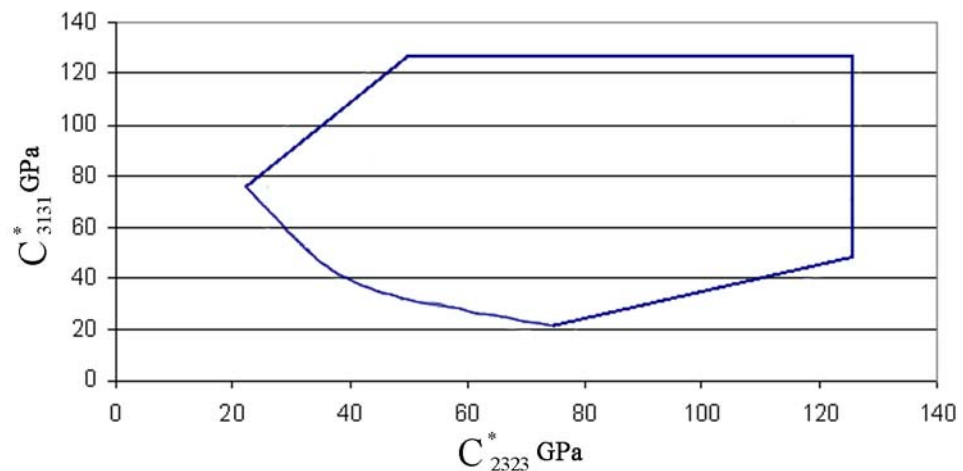


Figure A.12 Property closure of C_{2323}^* vs. C_{3131}^*

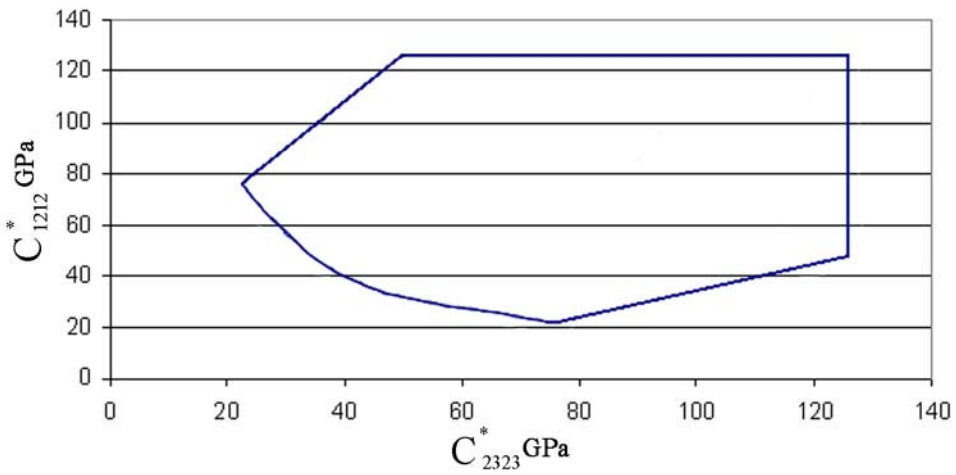


Figure A.13 Property closure of C^*_{2323} vs. C^*_{1212}

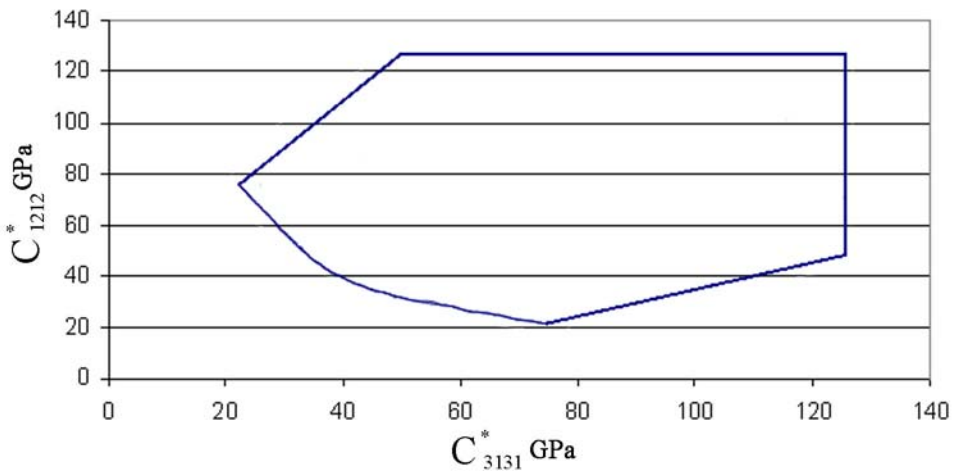


Figure A.14 Property closure of C^*_{3131} vs. C^*_{1212}

Appendix B : Inversion for cubic-orthorhombic symmetry

The following is an explicit inversion of the S'_{ij} tensor to the S'^{-1}_{ij} tensor. From equation (4.1) the S'_{ij} tensor is

$$\begin{bmatrix} S'_{11} & S'_{12} & S'_{13} & - & - & - \\ S'_{12} & S'_{22} & S'_{23} & - & - & - \\ S'_{13} & S'_{23} & S'_{33} & - & - & - \\ - & - & - & S'_{44} & - & - \\ - & - & - & - & S'_{55} & - \\ - & - & - & - & - & S'_{66} \end{bmatrix}. \quad (\text{H.1})$$

By using cofactors (H.1) is inverted by the following process.

$$S'^{-1}_{11} = \frac{S'_{22}S'_{33} - (S'_{23})^2}{S'_{11}S'_{22}S'_{33} + 2S'_{12}S'_{13}S'_{23} - S'_{22}(S'_{13})^2 - S'_{33}(S'_{12})^2 - S'_{11}(S'_{23})^2} \quad (\text{H.2})$$

$$S'^{-1}_{22} = \frac{S'_{11}S'_{33} - (S'_{13})^2}{S'_{11}S'_{22}S'_{33} + 2S'_{12}S'_{13}S'_{23} - S'_{22}(S'_{13})^2 - S'_{33}(S'_{12})^2 - S'_{11}(S'_{23})^2} \quad (\text{H.3})$$

$$S'^{-1}_{33} = \frac{S'_{11}S'_{22} - (S'_{12})^2}{S'_{11}S'_{22}S'_{33} + 2S'_{12}S'_{13}S'_{23} - S'_{22}(S'_{13})^2 - S'_{33}(S'_{12})^2 - S'_{11}(S'_{23})^2} \quad (\text{H.4})$$

$$S'^{-1}_{12} = \frac{-S'_{33}S'_{12} + S'_{13}S'_{23}}{S'_{11}S'_{22}S'_{33} + 2S'_{12}S'_{13}S'_{23} - S'_{22}(S'_{13})^2 - S'_{33}(S'_{12})^2 - S'_{11}(S'_{23})^2} \quad (\text{H.5})$$

$$S'^{-1}_{13} = \frac{S'_{12}S'_{23} - S'_{22}S'_{13}}{S'_{11}S'_{22}S'_{33} + 2S'_{12}S'_{13}S'_{23} - S'_{22}(S'_{13})^2 - S'_{33}(S'_{12})^2 - S'_{11}(S'_{23})^2} \quad (\text{H.6})$$

$$S_{23}'^{-1} = \frac{-S'_{11}S'_{23} + S'_{12}S'_{13}}{S'_{11}S'_{22}S'_{33} + 2S'_{12}S'_{13}S'_{23} - S'_{22}(S'_{13})^2 - S'_{33}(S'_{12})^2 - S'_{11}(S'_{23})^2} \quad (\text{H.7})$$

$$S_{44}'^{-1} = \frac{1}{S'_{44}} \quad (\text{H.8})$$

$$S_{55}'^{-1} = \frac{1}{S'_{55}} \quad (\text{H.9})$$

$$S_{66}'^{-1} = \frac{1}{S'_{66}} \quad (\text{H.10})$$

As can be seen equations (H.8), (H.9), and (H.10) are only a simple inverse and therefore produce a hyper-plane, and not a hyper-surface such as (H.2), (H.3), and (H.4).

Appendix C :Program for generation of the property closures

Property_C.c

```
/* property closer of <Cijkl> for the cubic orthorombic symmetry case
   , but only for Ciiii and Cijij
```

This program used a tie-line method for the material constants, but only a small changed was made to use discrete points from Hartley (). */

```
#include<stdio.h>
#include<stdlib.h>
#include<math.h>
#include<string.h>
#include"property.h"

/* these are where is is set which property closure to make */
#define C1 "C1111"
#define G1 "g1111"
#define K1 C1111
#define g1 g1111
#define C2 "C1212"
#define G2 "g1212"
#define K2 C1212
#define g2 g1212
#define PI 3.1415926
#define step PI / 25.0
#define N 1
#define ofiles "hartley_base.txt"
FILE *outfile;

void main()
{
    *****
        Initialize all variables
    *****
    int I = 1, J = 1, K = 1, M = 2, count = 0;
    double Land[N+3], landdumb, Ms, aa, bb;
    /* these are in dynes/cm^2 */
    /*double C111 = 1.684e12, C112 = 1.214e12, C144 = 0.754e12;
    double C211 = 2.465e12, C212 = 1.473e12, C244 = 1.247e12;*/
    /* these are in GPa */
    double C111 = 168.4, C112 = 121.4, C144 = 75.4; /* copper */
    double C211 = 246.5, C212 = 147.3, C244 = 124.7; /* nickel */

    double C1111, C2222, C3333, C2323, C3131, C1212, C1122, C1133, C2233;
    double a1111, a2222, a3333, a2323, a3131, a1212, a1122, a1133, a2233;
    double b1111, b2222, b3333, b2323, b3131, b1212, b1122, b1133, b2233;
    double g1111, g2222, g3333, g2323, g3131, g1212, g1122, g1133, g2233;
    double phi1, PHI, phi2;

    int pp, p, r;
    *****
    Open the output file and getGs loads in the orientations for a cubic euler space
    *****
    outfile = fopen(ofiles, "w");
```

```

*****
      Compute the composition variable by composition diversion set by N
*****
Ms = 1.0 / N;
Land[1] = Ms / 2.0;
Land[0] = 0.0;
landdumb = Land[1];
for(pp = 2; pp < N + 1; pp++) {
    landdumb = landdumb + Ms;
    Land[pp] = landdumb;
}
Land[N+1] = 1.0;
*****
Compute the variables that don't change with composition or orientation
*****
a1111 = Aijkm(1,1,1,1,C112,C144);
a2222 = Aijkm(2,2,2,2,C112,C144);
a3333 = Aijkm(3,3,3,3,C112,C144);
a2323 = Aijkm(2,3,2,3,C112,C144);
a3131 = Aijkm(3,1,3,1,C112,C144);
a1212 = Aijkm(1,2,1,2,C112,C144);
a1122 = Aijkm(1,1,2,2,C112,C144);
a1133 = Aijkm(1,1,3,3,C112,C144);
a2233 = Aijkm(2,2,3,3,C112,C144);

b1111 = Bijkm(1,1,1,1,C112,C144,C212,C244);
b2222 = Bijkm(2,2,2,2,C112,C144,C212,C244);
b3333 = Bijkm(3,3,3,3,C112,C144,C212,C244);
b2323 = Bijkm(2,3,2,3,C112,C144,C212,C244);
b3131 = Bijkm(3,1,3,1,C112,C144,C212,C244);
b1212 = Bijkm(1,2,1,2,C112,C144,C212,C244);
b1122 = Bijkm(1,1,2,2,C112,C144,C212,C244);
b1133 = Bijkm(1,1,3,3,C112,C144,C212,C244);
b2233 = Bijkm(2,2,3,3,C112,C144,C212,C244);

aa = C111 - C112 - (2.0 * C144);
bb = C211 - C111 + C112 - C212 + (2.0 * C144) - (2.0 * C244);

fprintf(outfile, "%s \t %s \t phi1 \t PHI \t phi2 \t %s \t %s \n",C1,C2,G1,G2);
*****
Find the minimum & maximum values for a set Ckmkm (which is the Y axes on the
property closure)
*****
for(p = 0; p < N + 2; p++) {
for(phi1 = 0.0001; phi1 <= 2 * PI; phi1+= step) {
for(PHI = 0.0001; PHI <= PI / 2.0; PHI+= step) {
for(phi2 = 0.0001; phi2 <= PI / 2.0; phi2+= step) {
C1111 = 0.0; C2222 = 0.0; C3333 = 0.0; C2323 = 0.0; C3131 = 0.0; C1212 = 0.0;
C1122 = 0.0; C1133 = 0.0; C2233 = 0.0;
g1111 = 0.0; g2222 = 0.0; g3333 = 0.0; g2323 = 0.0; g3131 = 0.0; g1212 = 0.0;
g1122 = 0.0; g1133 = 0.0; g2233 = 0.0;
*****
      This for loop calculates a value of Ckmkm
*****
for(r = 1; r < 4; r++) {

```

```

        C1111 += (aa + bb * Land[p]) * Gir(1,r,phi1,PHI,phi2) * Gir(1,r,phi1,PHI,phi2) *
Gir(1,r,phi1,PHI,phi2) * Gir(1,r,phi1,PHI,phi2);
        C2222 += (aa + bb * Land[p]) * Gir(2,r,phi1,PHI,phi2) * Gir(2,r,phi1,PHI,phi2) *
Gir(2,r,phi1,PHI,phi2) * Gir(2,r,phi1,PHI,phi2);
        C3333 += (aa + bb * Land[p]) * Gir(3,r,phi1,PHI,phi2) * Gir(3,r,phi1,PHI,phi2) *
Gir(3,r,phi1,PHI,phi2) * Gir(3,r,phi1,PHI,phi2);
        C2323 += (aa + bb * Land[p]) * Gir(2,r,phi1,PHI,phi2) * Gir(3,r,phi1,PHI,phi2) *
Gir(2,r,phi1,PHI,phi2) * Gir(3,r,phi1,PHI,phi2);
        C3131 += (aa + bb * Land[p]) * Gir(3,r,phi1,PHI,phi2) * Gir(1,r,phi1,PHI,phi2) *
Gir(3,r,phi1,PHI,phi2) * Gir(1,r,phi1,PHI,phi2);
        C1212 += (aa + bb * Land[p]) * Gir(1,r,phi1,PHI,phi2) * Gir(2,r,phi1,PHI,phi2) *
Gir(1,r,phi1,PHI,phi2) * Gir(2,r,phi1,PHI,phi2);
        C1122 += (aa + bb * Land[p]) * Gir(1,r,phi1,PHI,phi2) * Gir(1,r,phi1,PHI,phi2) *
Gir(2,r,phi1,PHI,phi2) * Gir(2,r,phi1,PHI,phi2);
        C1133 += (aa + bb * Land[p]) * Gir(1,r,phi1,PHI,phi2) * Gir(1,r,phi1,PHI,phi2) *
Gir(3,r,phi1,PHI,phi2) * Gir(3,r,phi1,PHI,phi2);
        C2233 += (aa + bb * Land[p]) * Gir(2,r,phi1,PHI,phi2) * Gir(2,r,phi1,PHI,phi2) *
Gir(3,r,phi1,PHI,phi2) * Gir(3,r,phi1,PHI,phi2);
        g1111 += Gir(1,r,phi1,PHI,phi2) * Gir(1,r,phi1,PHI,phi2) * Gir(1,r,phi1,PHI,phi2) *
Gir(1,r,phi1,PHI,phi2);
        g2222 += Gir(2,r,phi1,PHI,phi2) * Gir(2,r,phi1,PHI,phi2) * Gir(2,r,phi1,PHI,phi2) *
Gir(2,r,phi1,PHI,phi2);
        g3333 += Gir(3,r,phi1,PHI,phi2) * Gir(3,r,phi1,PHI,phi2) * Gir(3,r,phi1,PHI,phi2) *
Gir(3,r,phi1,PHI,phi2);
        g2323 += Gir(2,r,phi1,PHI,phi2) * Gir(3,r,phi1,PHI,phi2) * Gir(2,r,phi1,PHI,phi2) *
Gir(3,r,phi1,PHI,phi2);
        g3131 += Gir(3,r,phi1,PHI,phi2) * Gir(1,r,phi1,PHI,phi2) * Gir(3,r,phi1,PHI,phi2) *
Gir(1,r,phi1,PHI,phi2);
        g1212 += Gir(1,r,phi1,PHI,phi2) * Gir(2,r,phi1,PHI,phi2) * Gir(1,r,phi1,PHI,phi2) *
Gir(2,r,phi1,PHI,phi2);
        g1122 += Gir(1,r,phi1,PHI,phi2) * Gir(1,r,phi1,PHI,phi2) * Gir(2,r,phi1,PHI,phi2) *
Gir(2,r,phi1,PHI,phi2);
        g1133 += Gir(1,r,phi1,PHI,phi2) * Gir(1,r,phi1,PHI,phi2) * Gir(3,r,phi1,PHI,phi2) *
Gir(3,r,phi1,PHI,phi2);
        g2233 += Gir(2,r,phi1,PHI,phi2) * Gir(2,r,phi1,PHI,phi2) * Gir(3,r,phi1,PHI,phi2) *
Gir(3,r,phi1,PHI,phi2);
    }
    C1111 += a1111 + b1111 * Land[p];
    C2222 += a2222 + b2222 * Land[p];
    C3333 += a3333 + b3333 * Land[p];
    C2323 += a2323 + b2323 * Land[p];
    C3131 += a3131 + b3131 * Land[p];
    C1212 += a1212 + b1212 * Land[p];
    C1122 += a1122 + b1122 * Land[p];
    C1133 += a1133 + b1133 * Land[p];
    C2233 += a2233 + b2233 * Land[p];
    ++count;
    fprintf(outfile,"%lf %lf %lf %lf %lf %lf\n",K1, K2,phi1,PHI,phi2, g1, g2);
}
}
}
fprintf(stderr,"%i\n", p);
}
return;
}

```

Appendix D : Program for generation of the upper-bound

Upper.c

```
/* This program finds the hyperplanes for <CiJkm> */
#include<stdio.h>
#include<stdlib.h>
#include<math.h>
#include<string.h>
#include"property.h"
#define I 1
#define J 1
#define K 1
#define M 1
/* Set this value to find the hyperplane */
#define CiJkm 23.0e11
#define step 0.5
/* output files */
#define xfiles "C1111_x_23.txt"
#define yfiles "C1111_y_23.txt"
#define zfiles "C1111_z_23.txt"
#define ofiles "C1111_23 .txt"
FILE *xoutfile;
FILE *youtfile;
FILE *zoutfile;
FILE *outfile;
void main()
{
/* variabels */
double D1111[5][4],D2222[5][4],D3333[5][4],D1122[5][4],D1133[5][4],D2233[5][4],D2323[5][4],
D3131[5][4],D1212[5][4];
    double D[5][4], F411, F412, F413;
    double Kijkm, aa;
/* These are for copper and are in dynes/cm^2 */
    double C111 = 16.84e11, C112 = 12.14e11, C144 = 7.54e11;
/* these are for Nickel and are in dynes/cm^2 */
/* double C111 = 24.65e11, C112 = 14.73e11, C144 = 12.47e11; */
/* dummy variables */
int r = 0;
/* open files */
xoutfile = fopen(xfiles, "w");
youtfile = fopen(yfiles, "w");
zoutfile = fopen(zfiles, "w");
outfile = fopen(FILES, "w");
fprintf(stderr,"%i%i%i%i\n",I,J,K,M);
/* input the D coefficients that don't change with composition of same phase FCC */
D1111[0][1]= 0.599939; D1111[4][1]= 0.195980; D1111[4][2]= -0.292770; D1111[4][3]= 0.387240;
D2222[0][1]= 0.599939; D2222[4][1]= 0.195980; D2222[4][2]= 0.292770; D2222[4][3]= 0.387240;
D3333[0][1]= 0.599919; D3333[4][1]= 0.523168; D3333[4][2]= 0.000000; D3333[4][3]= 0.000000;
D1122[0][1]= 0.199980; D1122[4][1]= 0.065327; D1122[4][2]= 0.000000; D1122[4][3]= -0.387240;
D1133[0][1]= 0.200000; D1133[4][1]= -0.261861; D1133[4][2]= 0.292770; D1133[4][3]= 0.000000;
D2233[0][1]= 0.200000; D2233[4][1]= -0.261861; D2233[4][2]= -0.292770; D2233[4][3]= 0.000000;
D2323[0][1]= 0.200000; D2323[4][1]= -0.261861; D2323[4][2]= -0.292770; D2323[4][3]= 0.000000;
D3131[0][1]= 0.200000; D3131[4][1]= -0.261861; D3131[4][2]= 0.292770; D3131[4][3]= 0.000000;
D1212[0][1]= 0.199980; D1212[4][1]= 0.065327; D1212[4][2]= 0.000000; D1212[4][3]= -0.387240;
```

```

/* Assign the correct D coeff of the Cijkm */
if(I == 1 && J == 1 && K == 1 && M == 1) {
    D[0][1]=D1111[0][1]; D[4][1]=D1111[4][1]; D[4][2]=D1111[4][2]; D[4][3]=D1111[4][3];
}
if(I == 2 && J == 2 && K == 2 && M == 2) {
    D[0][1]=D2222[0][1]; D[4][1]=D2222[4][1]; D[4][2]=D2222[4][2]; D[4][3]=D2222[4][3];
}
if(I == 3 && J == 3 && K == 3 && M == 3) {
    D[0][1]=D3333[0][1]; D[4][1]=D3333[4][1]; D[4][2]=D3333[4][2]; D[4][3]=D3333[4][3];
}
if(I == 1 && J == 1 && K == 2 && M == 2) {
    D[0][1]=D1122[0][1]; D[4][1]=D1122[4][1]; D[4][2]=D1122[4][2]; D[4][3]=D1122[4][3];
}
if(I == 1 && J == 1 && K == 3 && M == 3) {
    D[0][1]=D1133[0][1]; D[4][1]=D1133[4][1]; D[4][2]=D1133[4][2]; D[4][3]=D1133[4][3];
}
if(I == 2 && J == 2 && K == 3 && M == 3) {
    D[0][1]=D2233[0][1]; D[4][1]=D2233[4][1]; D[4][2]=D2233[4][2]; D[4][3]=D2233[4][3];
}
if(I == 2 && J == 3 && K == 2 && M == 3) {
    D[0][1]=D2323[0][1]; D[4][1]=D2323[4][1]; D[4][2]=D2323[4][2]; D[4][3]=D2323[4][3];
}
if(I == 3 && J == 1 && K == 3 && M == 1) {
    D[0][1]=D3131[0][1]; D[4][1]=D3131[4][1]; D[4][2]=D3131[4][2]; D[4][3]=D3131[4][3];
}
if(I == 1 && J == 2 && K == 1 && M == 2) {
    D[0][1]=D1212[0][1]; D[4][1]=D1212[4][1]; D[4][2]=D1212[4][2]; D[4][3]=D1212[4][3];
}
Kijkm = Aijkm(I,J,K,M,C112,C144);
aa = C111 - C112 - (2.0 * C144);
fprintf(outfile, "C%i%i%i%i\n F411\t F412\t F413\n",I,J,K,M);
/* Compute points on a plane */
for(F412 = -8; F412 <= 8; F412 += step) {
    fprintf(stderr,"F411 = %f\n",F412);
    for(F411 = -5.0; F411 <= 7.0; F411 += step) {
        F413 = (9.0 / D[4][3]) * (((Cijkm - Kijkm) / aa) - (D[0][1] + ((D[4][1] * F411) / 9) +((D[4][2] * F412) / 9)));
        fprintf(xoutfile, "%f\t",F411);
        fprintf(youtfile, "%f\t",F412);
        fprintf(zoutfile, "%f\t",F413);
        fprintf(outfile, "%f\t %f\t %f\n",F411, F412, F413);
    }
    fprintf(xoutfile,"\\n");
    fprintf(youtfile,"\\n");
    fprintf(zoutfile,"\\n");
}
fclose(xoutfile);
fclose(youtfile);
fclose(zoutfile);
fclose(outfile);
return;
}

```

Appendix E : Program for generation of the lower-bound

Lower.c

```
/* Lower bound for Siiii and Sijij of <S>-1 of ijkm */

#include<stdio.h>
#include<stdlib.h>
#include<math.h>
#include<string.h>
#include"property.h"

/*this sets what lower bound is found */
#define I 1
#define J 1
#define K 1
#define M 1
/* This sets the value of the hyper surface to be found */
#define Sset 20.0e11
#define tol 1.0e6
#define Step 1.0
#define PI 3.141593
#define ofiles "S1111_1.txt"
#define sxfile "S1111_x_20.txt"
#define syfile "S1111_y_20.txt"
#define szfile "S1111_z_20.txt"
FILE *outfile;
FILE *xfile;
FILE *yfile;
FILE *zfile;

void main()
{
/* variabels */
    double
D1111[5][4],D2222[5][4],D3333[5][4],D1122[5][4],D1133[5][4],D2233[5][4],D2323[5][4],D3131[5][4]
],D1212[5][4], D[5][4];
    double K1111, K2222, K3333, K1122, K1133, K2233, K2323, K3131, K1212;
    double S1111, S2222, S3333, S1122, S1133, S2233, S2323, S3131, S1212;
    double Sijkm = 0.0, F411, F412, F413, Fset, Fcenter;
    double aa, det, Kijk, aaK, Cijk;
    /* These are for copper */
    double S111 = 1.498e-12, S112 = -0.629e-12, S144 = 1.326e-12 / 4.0;
    double C111 = 16.84e11, C112 = 12.14e11, C144 = 7.54e11;
    /* these are for Nickel */
    /* double S111 = 0.734e-12, S112 = -0.274e-12, S144 = 0.802e-12; */

    fprintf(stderr,"S%ii%ii%ii%i\n",I,J,K,M);

/* open files need and load T files */
    outfile = fopen(ofiles, "w");
    xfile = fopen(sxfile, "w");
    yfile = fopen(syfile, "w");
    zfile = fopen(szfile, "w");
```

```

K1111 = Aijkm(1,1,1,1,S112,S144);
K2222 = Aijkm(2,2,2,2,S112,S144);
K3333 = Aijkm(3,3,3,3,S112,S144);
K1122 = Aijkm(1,1,2,2,S112,S144);
K1133 = Aijkm(1,1,3,3,S112,S144);
K2233 = Aijkm(2,2,3,3,S112,S144);
K2323 = Aijkm(2,3,2,3,S112,S144);
K3131 = Aijkm(3,1,3,1,S112,S144);
K1212 = Aijkm(1,2,1,2,S112,S144);
Kijkm = Aijkm(I,J,K,M,C112,C144);

aa = S111 - S112 - (2.0 * S144);
aaK = C111 - C112 - (2.0 * C144);

/* input the D coefficients that don't change with phase */
D1111[0][1]= 0.599939; D1111[4][1]= 0.195980; D1111[4][2]=-0.292770; D1111[4][3]= 0.38724;
D2222[0][1]= 0.599939; D2222[4][1]= 0.195980; D2222[4][2]= 0.292770; D2222[4][3]= 0.38724;
D3333[0][1]= 0.599919; D3333[4][1]= 0.523168; D3333[4][2]= 0.000000; D3333[4][3]= 0.00000;
D1122[0][1]= 0.199980; D1122[4][1]= 0.065327; D1122[4][2]= 0.000000; D1122[4][3]=-0.38724;
D1133[0][1]= 0.200000; D1133[4][1]=-0.261861; D1133[4][2]= 0.292770; D1133[4][3]= 0.00000;
D2233[0][1]= 0.200000; D2233[4][1]=-0.261861; D2233[4][2]=-0.292770; D2233[4][3]= 0.00000;
D2323[0][1]= 0.200000; D2323[4][1]=-0.261861; D2323[4][2]=-0.292770; D2323[4][3]= 0.00000;
D3131[0][1]= 0.200000; D3131[4][1]=-0.261861; D3131[4][2]= 0.292770; D3131[4][3]= 0.00000;
D1212[0][1]= 0.199980; D1212[4][1]= 0.065327; D1212[4][2]= 0.000000; D1212[4][3]=-0.38724;

/* Assign the correct D coeff of the Cijkm */
if(I == 1 && J == 1 && K == 1 && M == 1) {
    D[0][1]=D1111[0][1]; D[4][1]=D1111[4][1]; D[4][2]=D1111[4][2]; D[4][3]=D1111[4][3];
}
if(I == 2 && J == 2 && K == 2 && M == 2) {
    D[0][1]=D2222[0][1]; D[4][1]=D2222[4][1]; D[4][2]=D2222[4][2]; D[4][3]=D2222[4][3];
}
if(I == 3 && J == 3 && K == 3 && M == 3) {
    D[0][1]=D3333[0][1]; D[4][1]=D3333[4][1]; D[4][2]=D3333[4][2]; D[4][3]=D3333[4][3];
}
if(I == 1 && J == 1 && K == 2 && M == 2) {
    D[0][1]=D1122[0][1]; D[4][1]=D1122[4][1]; D[4][2]=D1122[4][2]; D[4][3]=D1122[4][3];
}
if(I == 1 && J == 1 && K == 3 && M == 3) {
    D[0][1]=D1133[0][1]; D[4][1]=D1133[4][1]; D[4][2]=D1133[4][2]; D[4][3]=D1133[4][3];
}
if(I == 2 && J == 2 && K == 3 && M == 3) {
    D[0][1]=D2233[0][1]; D[4][1]=D2233[4][1]; D[4][2]=D2233[4][2]; D[4][3]=D2233[4][3];
}
if(I == 2 && J == 3 && K == 2 && M == 3) {
    D[0][1]=D2323[0][1]; D[4][1]=D2323[4][1]; D[4][2]=D2323[4][2]; D[4][3]=D2323[4][3];
}
if(I == 3 && J == 1 && K == 3 && M == 1) {
    D[0][1]=D3131[0][1]; D[4][1]=D3131[4][1]; D[4][2]=D3131[4][2]; D[4][3]=D3131[4][3];
}
if(I == 1 && J == 2 && K == 1 && M == 2) {
    D[0][1]=D1212[0][1]; D[4][1]=D1212[4][1]; D[4][2]=D1212[4][2]; D[4][3]=D1212[4][3];
}

/* start finding the F411, F412, F413 to form the hyper-curve */
fprintf(outfile,"S%i%j%k%l%t F411%t F412%t F413%t Fcenter\n", I,J,K,M);

```

```

for(F412 = -8.0; F412 <= 8.0; F412 += Step) {
    fprintf(stderr,"F412 = %f\n",F412);
    for(F411 = -6.0; F411 <= 8.0; F411 += Step) {
        F411 = -0.1447497; F412 = 0.04706759; F413 = -0.2128656;
        Fcenter = (9.0 / D[4][3]) * (((Sset - Kijkm) / aaK) - (D[0][1] + ((D[4][1] *
        F411) / 9) + ((D[4][2] * F412) / 9)));
        Cijkm = Kijkm + aaK * (D[0][1] + ((D[4][1] * F411) / 9.0) + ((D[4][2] * F412) /
        9.0) + ((D[4][3] * Fcenter) / 9.0));
        Fset = Fcenter + 30.0;
        for(F413 = Fcenter - 30.0; F413 <= Fset; F413 += 0.00001) {
            F411 = -0.1447497; F412 = 0.04706759; F413 = -0.2128656;
            S1111 = K1111 + aa * (D1111[0][1] + (D1111[4][1] / 9.0) * F411
            + (D1111[4][2] / 9.0) * F412
            + (D2222[4][2] / 9.0) * F412
            + (D3333[4][2] / 9.0) * F412
            + (D1122[4][2] / 9.0) * F412
            + (D1133[4][2] / 9.0) * F412
            + (D2233[4][2] / 9.0) * F412
            + (D2323[4][2] / 9.0) * F412
            + (D3131[4][2] / 9.0) * F412
            + (D1212[4][2] / 9.0) * F412
            (S2222 * S1133 * S1133)
            /* S1111 */
            if(I == 1 && J == 1 && K == 1 && M == 1) {
                Sijkm = ((S2222 * S3333) - (S2233 * S2233)) / det;
            }
            /* S2222 */
            if(I == 2 && J == 2 && K == 2 && M == 2) {
                Sijkm = ((S1111 * S3333) - (S1133 * S1133)) / det;
            }
            /* S3333 */
            if(I == 3 && J == 3 && K == 3 && M == 3) {
                Sijkm = ((S1111 * S2222) - (S1122 * S1122)) / det;
            }
            /* S1122 */
            if(I == 1 && J == 1 && K == 2 && M == 2) {
                Sijkm = ((-1 * S3333 * S1122) + (S1133 * S2233)) / det;
            }
            /* S1133 */
            if(I == 1 && J == 1 && K == 3 && M == 3) {
                Sijkm = ((S1111 * S2222) - (S1122 * S1122)) / det;
            }
        }
    }
}

```

```

                Sijkm = ((S1122 * S2233) - (S2222 * S1133)) / det;
            }
/* S2233 */        if(I == 2 && J == 2 && K == 3 && M == 3) {
                Sijkm = (-1 * (S1111 * S2233) + (S1122 * S1133)) / det;
            }
/* S2323 */        if(I == 2 && J == 3 && K == 2 && M == 3) {
                Sijkm = 1.0 / S2323;
            }
/* S3131 */        if(I == 3 && J == 1 && K == 3 && M == 1) {
                Sijkm = 1.0 / S3131;
            }
/* S1212 */        if(I == 1 && J == 2 && K == 1 && M == 2) {
                Sijkm = 1.0 / S1212;
            }

            if(Sijkm <= Sset + tol && Sijkm >= Sset - tol) {
                fprintf(outfile, "%e\t %f\t %f\t %f\n", Sijkm, F411, F412, F413, Fcenter);

                fprintf(xfile,"%f",F411);
                fprintf(yfile,"%f",F412);
                fprintf(zfile,"%f",F413);
            }
        }
    }
    fprintf(xfile, "\n");
    fprintf(yfile, "\n");
    fprintf(zfile, "\n");
}

fclose(outfile);
fclose(xfile);
fclose(yfile);

fclose(zfile);

return;
}

```

Appendix F : Program for computing the ${}^\phi D_{lr}^{*1\eta}$ coefficients

D_coeff.c

```

/* this finds the D coefficients need by the other programs */
#include<stdio.h>
#include<stdlib.h>
#include<math.h>
#include<string.h>
#include"property.h"
#include"harmonics.h"

#define I 1
#define J 1
#define K 1
#define M 1
#define L 4
#define n 3
#define step PI / 100
/* #define PI 3.141593 // from harmonics.h file */
#define ofiles "D_1111.txt"
FILE *outfile;

void main()
{
/* variabels */
    double D[5][4], test, phi1, phi2, PHI, Gs;
    double factor;

/* dummy variables */
    int r;

/* open files need and load T files */
    outfile = fopen(ofiles, "w");
    getFourieras();
    getCubicBs();

    factor = 1.0 / (8.0 * PI * PI);

    test = 0.0;
    D[0][1] = 0.0; D[4][1] = 0.0; D[4][2] = 0.0; D[4][2] = 0.0;

    for(phi1 = 0.0001; phi1 <= 2 * PI; phi1 += step) {
        for(PHI = 0.0001; PHI <= PI; PHI += step) {
            for(phi2 = 0.0001; phi2 <= 2.0 * PI; phi2 += step) {
                test += CubLowerT(4,1,n,phi1,PHI,phi2).re * CubLowerT(4,1,n,phi1,PHI,phi2).re * sin(PHI) *
factor * (step * step * step);
                Gs = 0.0;
                for(r = 1; r < 4; r++) {
                    Gs += Gir(I,r,phi1,PHI,phi2) * Gir(J,r,phi1,PHI,phi2) * Gir(K,r,phi1,PHI,phi2) *
Gir(M,r,phi1,PHI,phi2);
                }
                D[0][1] += Gs * factor * sin(PHI) * (step * step * step);
                D[L][1] += Gs * factor * sin(PHI) * (step * step * step) * CubLowerT(L,1,1,phi1,PHI,phi2).re;
                D[L][2] += Gs * factor * sin(PHI) * (step * step * step) * CubLowerT(L,1,2,phi1,PHI,phi2).re;
            }
        }
    }
}

```

```

D[L][3] += Gs * factor * sin(PHI) * (step * step * step) * CubLowerT(L,1,3,phi1,PHI,phi2).re;
}
}

fprintf(stderr, "T41%i intergration = %lf\n",n,9 * test);
/* times in the 2l+1 factor */
D[0][1] = D[0][1] * (2.0 * 0 + 1.0);
D[L][1] = D[L][1] * (2.0 * L + 1.0);
D[L][2] = D[L][2] * (2.0 * L + 1.0);
D[L][3] = D[L][3] * (2.0 * L + 1.0);
fprintf(stderr, "D011 = %lf\t D411 = %lf\t D412 = %lf\t D413 = %lf\n",D[0][1],D[L][1],D[L][2],D[L][3]);
fprintf(outfile, "C%i%i%i%i D coefficients \n",I,J,K,M);
fprintf(outfile, "D011 = %lf\t D411 = %lf\t D412 = %lf\t D413 = %lf\n",D[0][1],D[L][1],D[L][2],D[L][3]);

fclose(outfile);

return;
}

```

Appendix G : Harmonics.h subroutine

Harmonics.h

```
/*
 * This library of routines contains functions for calculating an ODF using a
 * Generalized Spherical Harmonic Series Expansion (GSHE) from single orientation
 * measurements existing in the form of orientation matrices. Unless otherwise noted
 * the mathematics for the code are found in:
 *
 * H.J. Bunge, Texture Analysis in Materials Science. Butterworths, London (1982)
 *
 * Stuart Wright, Yale University (1991).
 *
 * Pole Figures routines have been added. The output and inputs for these routines
 * are formatted according to popLA conventions.
 *
 * Stuart Wright, Los Alamos National Lab (1993).
 */
/* -----
 * The U.S. Government is licensed to use, reproduce, and distribute this software.
 * Permission is granted to the public to copy and use these portions of the software
 * without charge, provided that this notice and the following statement of authorship
 * are reproduced in all copies.
 *
 * Neither the U.S. Government nor S. I. Wright makes any warranty, express or
 * implied, or assumes liability or responsibility for the use of this software.
 *
 */
/* -----
 * The following is an initializing routine required before using any of the
 * GSHE routines. It returns an error code according to the following:
 * 0: No errors encountered.
 *      1: Invalid symmetry combination.
 *      2: Problem reading Cubic symmetry coefficients.
 *      3: Problem reading Fourier Coefficients.
 *          4: Not enough memory to allocate arrays.
 *          5: Not enough memory for Taylor Factor calculations.
 *
 * cv: Verbose - show error messages
 * l: Rank for harmonic expansions
 * Csym: Crystal Symmetry
 * Psym: Processing, sample or statistical symmetry
 * EXAMPLE: GSHEInit(1,16,cubic,triclinic)
 */
/* Portions of the above mentioned software is included in the file harmonics.h*/
/* Functions
```

getFourieras(void), getCubicBs(void) -

Load tables of values required for all other functions.

```
complex kfnc(int l, int m, double phi, double beta) -  
    Calculates surface spherical harmonic functions without symmetry.  
  
double kcfcfnc(int l, int m, double phi, double beta) -  
    Calculates surface spherical harmonic functions with cubic crystal symmetry.  
  
complex CubTriclT(int l,int mu,int nu,float phi1,float PHI,float phi2) -  
    This function calculates the T functions with cubic-triclinic symmetry.  
  
complex TriLowerT(int l,int mu,int nu,float phi1,float PHI,float phi2) -  
    This function calculates the T functions when the crystal is triclinic  
    and the right-hand symmetry is lower.  
  
complex LowerTriT(int l,int mu,int nu,float phi1,float PHI,float phi2) -  
    This function calculates the T functions when the right-hand symmetry is  
    triclinic and the crystal symmetry is lower.  
  
complex LowLowerT(int l,int mu,int nu,float phi1,float PHI,float phi2) -  
    This function calculates the T functions when both symmetries are lower.  
    (Bunge eqn. (14.258)).  
  
complex CubLowerT(int l,int mu,int nu,float phi1,float PHI,float phi2) -  
    This function calculates the T functions when the processing symmetry is 'low'  
    and the crystal symmetry is 'high' (cubic) (Bunge eqn. (14.261)).  
  
complex CubCubicT(int l,int mu,int nu,float phi1,float PHI,float phi2) -  
    This function calculates the T functions cubic-cubic symmetry  
    (Bunge eqn. (14.271)).  
  
complex TriTriclT(int l,int mu,int nu,float phi1,float PHI,float phi2) -  
    This function calculates the T functions when both symmetries are triclinic.
```

*/

```
#include<stdio.h>  
#include<stdlib.h>  
#include<string.h>  
#include<time.h>  
#include<math.h>  
#define rank 34  
#define triclinic      0  
#define orthorhombic  11  
#define orthotropic   11  
#define tetragonal    12  
#define hexagonal     13  
#define axial         14  
#define monoclinic   15  
#define trigonal      20  
#define cubic         1  
#define PI            3.1415926535897931  
#define sign(l)        (((l)%2) ? -1:1)  
#define sq2pi         2.506628274631
```

```

#define sq2          1.414213562373
typedef struct complex
{
    double re;
    double im;
} complex;

double B[35][9][4];
double a[35][35][35][35];
char path[200];
double sinPHI[50];
double cosPHI[50];

int      processSym,crystalSym, *M,*N ,SymCombo,bsize;

/*getFourieras function from GSHELlib.c from Stuart Wright*/
/* -----
 * The following function reads in the Fourier coefficients (a'l'mns) from file almns.
 * It returns a = 1 if successful.
 * ----- */
int getFourieras(void) {
    FILE    *asFile;
    int      l,m,n,s;
    double  almns;

    /* read in Fourier coefficients from file almns */
    asFile = fopen("almns", "r");
    if (!asFile) return 0;
    for (l=0; l<rank; ++l) {
        for (m=0; m<=l; ++m) for (n=0; n<=m; ++n) for (s=0; s<=l; ++s) {
            if(fscanf(asFile, "%lf", &almns)==EOF) return(0);
            a[l][m][n][s] = almns;
            a[l][n][m][s] = almns;
        }
    }
    fclose(asFile);
    return 1;
}

/*getCubicBs function from GSHELlib.c from Stuart Wright*/
/* -----
 * The following function reads in the cubic symmetry coefficients (Bl4mn) from file
 * CubicBs. It returns a = 1 if successful.
 * ----- */
int getCubicBs()
{
    FILE    *BsFile;
    int      l,m,n;
    double  Blmn;

    /* read in cubic symmetry coefficients from file CubicBs */

    BsFile = fopen("CubicBs", "r");
    if (!BsFile) return 0;
    for (;;) {

```

```

        if (fscanf(BsFile,"%i %i %i %lf",&l,&m,&n,&Blmn)==EOF) break;
        if (l > rank) break;
        B[l][m][n] = Blmn;
    }
    fclose(BsFile);
    return 1;
}

double Pfnc(int m, int l, double phi)
{
    int mevent,moddt,s,slevent,sloddt;
    int m2event,m2oddt;
    double anpc,asnpc,asp;
    double rv;
    double angl;

    rv=0;
    mevent= (m / 2.0) +.1;
    moddt= (m / 2.0) +.9;
    if(mevent==moddt)
    {
        for(s=0;s<=l;s++)
        {
            anpc=a[l][m][0][s];
            slevent= ((l+s) / 2.0) +.1;
            sloddt= ((l+s) / 2.0) +.9;
            m2event= (m / 4.0) +.1;
            m2oddt= (m / 4.0) +.9;
            if(m2event==m2oddt)asnpc= anpc / (sqrt((2.0 / (2 * l + 1))));
            if(m2event!=m2oddt)asnpc= (-anpc) / (sqrt((2.0 / (2 * l + 1))));
            if(slevent==sloddt)asp=asnpc;
            if(slevent!=sloddt)asp=0;
            angl=(s * phi);
            rv+=(asp * (cos(angl)));
        }
    }
    if(mevent!=moddt)
    {
        for(s=0;s<=l;s++)
        {
            anpc=a[l][m][0][s];
            slevent= ((l+s) / 2.0) +.1;
            sloddt= ((l+s) / 2.0) +.9;
            m2event= ((m-1) / 4.0) +.1;
            m2oddt= ((m-1) / 4.0) +.9;
            if(m2event==m2oddt)asnpc= (-anpc) / (sqrt((2.0 / (2 * l + 1))));
            if(m2event!=m2oddt)asnpc= (anpc) / (sqrt((2.0 / (2 * l + 1))));
            if(slevent==sloddt)asp=asnpc;
            if(slevent!=sloddt)asp=0;
            angl=(s * phi);
            rv+=(asp * (sin(angl)));
        }
        rv=-rv;
    }
    return(rv);
}

```

```

}

complex kfnc(int l, int m, double phi, double beta)
{
    complex value1,value3;
    double value2;
    int me,mo;
    me=getCubicBs();
    mo=getFourieras();
    value2=Pfnc(m,l,phi);
    value1.re=((cos (m * beta)) / sqrt((2 * PI)));
    value1.im=((sin (m * beta)) / sqrt((2 * PI)));
    me= (m / 2.0) +.1;
    mo= (m / 2.0) +.9;
    if(me==mo)
    {
        value3.re=value1.re * value2;
        value3.im=value1.im * value2;
    }
    if(me!=mo)
    {
        value3.re=value1.re * value2;
        value3.im=value1.im * value2;
        /*value3.re=(-1 * value1.im * value2);
        value3.im=(value1.re * value2);*/
    }
    return(value3);
}

double kcpcfnc(int l, int m, double phi, double beta)
{
    int n;
    double rv;
    int ne ,no ;
    rv=0;
    for(n=0;n<=l;n++)
    {
        /*ne = (n / 2.0) +.1;
        no = (n / 2.0) +.9;
        if(ne==no) rv.re+=(B[l][n][m] * Pfnc(n,l,phi) * cos((n * beta)));
        if(ne!=no) rv.im+=(B[l][n][m] * Pfnc(n,l,phi) * cos((n * beta)));
        ne= ((n) / 4.0) + .1;
        no= ((n) / 4.0) + .9;
        if(ne==no) rv+=(B[l][ne][m] * Pfnc(n,l,phi) * cos((n * beta)));
        */
        return(rv);
    }
}

/*
 * This function calculates the T functions cubic-triclinic symmetry.
 */
complex CubTricT(int l,int mu,int nu,float phi1,float PHI,float phi2)
{

```

```

complex Tlmn,R;
int m,s;
float cc,cs,ss,sc,cnp1,snp1,cmp2,smp2;
double sum1,sum2;
double sinPHI[50];
double cosPHI[50];

Tlmn.re = 1;
Tlmn.im = 0;
if (l==0) return Tlmn;

/* --- Attempt to speed up calculations --- */

Tlmn.im = Tlmn.re = 0;
cnp1 = (float) cos(nu * phi1);
snp1 = (float) sin(nu * phi1);

if ((nu%2)!=0)
{
    for (s=1; s<=l; ++s) sinPHI[s] = sin(s * PHI);
    for (m=0; m<=l; m+=4)

    {
        sum1 = sum2 = 0.0;
        cmp2 = (float) cos(m * phi2);
        smp2 = (float) sin(m * phi2);
        cc = cmp2 * cnp1;
        ss = smp2 * snp1;
        sc = smp2 * cnp1;
        cs = cmp2 * snp1;
        for (s=2; s<=l; s+=2) sum1 += a[l][m][nu][s] * sinPHI[s];
        for (s=1; s<=l; s+=2) sum2 += a[l][m][nu][s] * sinPHI[s];
        R.re = -cs * sum1 -sc * sum2;
        R.im = cc * sum1 - ss * sum2;
        Tlmn.re += (B[l][m/4][mu] * R.re);
        Tlmn.im += (B[l][m/4][mu] * R.im);
    }
}

} else
{
    for (s=0; s<=l; ++s) cosPHI[s] = cos(s * PHI);
    for (m=0; m<=l; m+=4)

    {
        sum1 = sum2 = 0.0;
        cmp2 = (float) cos(m * phi2);
        smp2 = (float) sin(m * phi2);
        cc = cmp2 * cnp1;
        ss = smp2 * snp1;
        sc = smp2 * cnp1;

```

```

        cs = cmp2 * snp1;
        for (s=0; s<=l; s+=2) sum1 += a[l][m][nu][s] * cosPHI[s];
        for (s=1; s<=l; s+=2) sum2 += a[l][m][nu][s] * cosPHI[s];
        R.re = cc * sum1 - ss * sum2;
        R.im = cs * sum1 + sc * sum2;
        Tlmn.re += (B[l][m/4][mu] * R.re);
        Tlmn.im += (B[l][m/4][mu] * R.im);

    }

}

Tlmn.re *= sq2pi;
Tlmn.im *= sq2pi;

return Tlmn;
}

/*
* This function maps the mu or nu indices to the corresponding m or n value
* for triclinic symmetry.
*/
int TriMap(int mu)
{
    if (mu%2) return (mu+1)/2;
    else return -mu/2;
}

complex noSymT(int l, int m, int n, float phi1, float PHI, float phi2)
{
    complex Tlmn;
    double sum1=0,cc,ss,cs,sc;
    int s,mp,np;

    mp = abs(m);
    np = abs(n);
    cc = cos(n * phi1) * cos(m * phi2);
    ss = sin(n * phi1) * sin(m * phi2);
    cs = cos(n * phi1) * sin(m * phi2);
    sc = sin(n * phi1) * cos(m * phi2);

    if (!((mp+np)%2))
    { /* --- m+n even --- */
        if (m * n<0) for (s=0; s<=l; ++s) sum1 += sign(l+s) * a[l][mp][np][s] * cos(s * PHI);
        else for (s=0; s<=l; ++s) sum1 += a[l][mp][np][s] * cos(s * PHI);
        Tlmn.re = (cc - ss) * sum1;
        Tlmn.im = (cs + sc) * sum1;
    } else
    { /* --- m+n odd --- */
        if (m * n<0) for (s=0; s<=l; ++s) sum1 += sign(l+s) * a[l][mp][np][s] * sin(s * PHI);
        else for (s=0; s<=l; ++s) sum1 += a[l][mp][np][s] * sin(s * PHI);
        Tlmn.im = (cc - ss) * sum1;
        Tlmn.re = -(cs + sc) * sum1;
    }
    return Tlmn;
}

```

```

/*
 * This function calculates the Slmn functions (Bunge eqn. (14.257)).
 */
complex Slmn(int l, int m, int n, float phi1, float PHI, float phi2)
{
    double sum1=0.0,sum2=0.0,cc,ss;
    complex rS;
    int s;

    rS.re = 0.0;
    rS.im = 0.0;
    cc = cos(n * phi1) * cos(m * phi2);
    ss = sin(n * phi1) * sin(m * phi2);

    for (s=0; s<=l; s+=2) sum1 += a[l][m][n][s] * cos(s*PHI);
    for (s=1; s<=l; s+=2) sum2 += a[l][m][n][s] * cos(s*PHI);
    rS.re = sum1 * cc - sum2 * ss;
    return rS;
}

complex Rlmn(int l, int m, int n, float phi1, float PHI, float phi2)
{
    complex R;
    double sum1=0,sum2=0,cc,ss,cs,sc,cnp1,snp1,cmp2,smp2;
    int s,lf,np;

    cnp1 = cos(n * phi1);
    snp1 = sin(n * phi1);
    cmp2 = cos(m * phi2);
    smp2 = sin(m * phi2);
    cc = cnp1 * cmp2;
    ss = snp1 * smp2;
    cs = cnp1 * smp2;
    sc = snp1 * cmp2;
    /* cc = cos(n * phi1) * cos(m * phi2);
    ss = sin(n * phi1) * sin(m * phi2);
    cs = cos(n * phi1) * sin(m * phi2);
    sc = sin(n * phi1) * cos(m * phi2); */

    if (n%2)
    { /* --- n odd --- */
        if (n>=0)
        {
            /* for (s=0; s<=l; s+=2) sum1 += a[l][m][n][s] * sin(s * PHI); */
            for (s=2; s<=l; s+=2) sum1 += a[l][m][n][s] * sin(s * PHI);
            for (s=1; s<=l; s+=2) sum2 += a[l][m][n][s] * sin(s * PHI);
        } else
        {
            lf = sign(l); np = abs(n);
            /*
            for (s=0; s<=l; s+=2) sum1 += lf * a[l][m][np][s] * sin(s * PHI);
            for (s=2; s<=l; s+=2) sum1 += lf * a[l][m][np][s] * sin(s * PHI);
            lf *= -1;
            for (s=1; s<=l; s+=2) sum2 += lf * a[l][m][np][s] * sin(s * PHI);
            */
        }
    }
}

```

```

        for (s=2; s<=l; s+=2) sum1 += a[l][m][np][s] * sin(s * PHI);
        for (s=1; s<=l; s+=2) sum2 += a[l][m][np][s] * sin(s * PHI);
        sum1 *= lf;
    sum2 *= (-lf);
}
R.re = -sc * sum1 -cs * sum2;
R.im = cc * sum1 - ss * sum2;

} else
{ /* --- n even --- */
    if (n>=0)
{
    for (s=0; s<=l; s+=2) sum1 += a[l][m][n][s] * cos(s * PHI);
    for (s=1; s<=l; s+=2) sum2 += a[l][m][n][s] * cos(s * PHI);
} else
{
    lf = sign(l); np = abs(n);
/*
for (s=0; s<=l; s+=2) sum1 += lf * a[l][m][np][s] * cos(s * PHI);
lf *= -1;
for (s=1; s<=l; s+=2) sum2 += lf * a[l][m][np][s] * cos(s * PHI);
*/
for (s=0; s<=l; s+=2) sum1 += a[l][m][np][s] * cos(s * PHI);
for (s=1; s<=l; s+=2) sum2 += a[l][m][np][s] * cos(s * PHI);
sum1 *= lf;
sum2 *= (-lf);
}
R.re = cc * sum1 - ss * sum2;
R.im = sc * sum1 + cs * sum2;
}
return R;
}

/*
* This function calculates the normalization factors (Bunge eqns.(14.259) and (14.260).
*/
float normFactor(int symmetry,int l,int mu,int *m)
{
    int Z;
    if (symmetry==axial)
{
    *m = 0;
    if (mu==1) return 1;
    else return 0;
} else {
    if (symmetry==orthorhombic)    Z = 2;
    if (symmetry==tetragonal)      Z = 4;
    if (symmetry==hexagonal)       Z = 6;
}
/* if ((l%2) *m = Z*mu; */ /* is this really true? otherwise Rlmn = 0 */
/* else *m = Z*(mu-1); */ /* for l=7,9,11 and 13 for hexagonal symmetry. */
*m = Z * (mu-1);           /* however, this is what the red bible says! */
if (*m==0) return 1;
else return (float) 1.414213562; /* square root of 2 */
}

```

```

/*Complex addition*/
complex cx_add(complex AAA, complex BBB)
{
    complex CCC;
    CCC.re = AAA.re + BBB.re;
    CCC.im = AAA.im + BBB.im;
    return(CCC);
}

/*
* This function calculates the T functions when the crystal is triclinic
* and the right-hand symmetry is lower.
*/
complex TriLowerT(int l,int mu,int nu,float phi1,float PHI,float phi2)
{
    complex Tlmn;
    float En;
    int mup,n;
    mup = TriMap(mu);

    En = normFactor(processSym,l,nu,&n);
    Tlmn = cx_add(noSymT(l,mup,n,phi1,PHI,phi2),noSymT(l,mup,-n,phi1,PHI,phi2));
    Tlmn.re *= En;
    Tlmn.im *= En;
    return Tlmn;
}
/*
* This function calculates the T functions when the right-hand symmetry is triclinic
* and the crystal symmetry is lower.
*/
complex LowerTriT(int l,int mu,int nu,float phi1,float PHI,float phi2)
{
    complex Tlmn;
    float Em;
    int mup;
    Em = normFactor(crystalSym,l,mu,&mup);
    Tlmn = Rlmn(l,mup,nu,phi1,PHI,phi2);
    Tlmn.re *= Em/2.0;
    Tlmn.im *= Em/2.0;
    return Tlmn;
}
/*
* This function calculates the T functions when both symmetries are lower.
* (Bunge eqn. (14.258)).
*/
complex LowLowerT(int l,int mu,int nu,float phi1,float PHI,float phi2)
{
    complex Tlmn;
    float En,Em;
    int m,n;
    Em = normFactor(crystalSym,l,mu,&m);
    En = normFactor(processSym,l,nu,&n);
    fprintf(stderr,"Test 1");
    Tlmn = Slmn(l,m,n,phi1,PHI,phi2);
    Tlmn.re *= (Em * En);
}

```

```

Tlmn.im *= (Em * En);
    return Tlmn;
}
/* -----
* This function calculates the T functions when the processing symmetry is 'low'
* and the crystal symmetry is 'high' (cubic) (Bunge eqn. (14.261)).
* -----
complex CubLowerT(int l,int mu,int nu,float phi1,float PHI,float phi2)
{
    complex Tlmn,S;
    int      n,m;
    float   En,sqt2PI;

    sqt2PI = (float) 2.506628275;
    En = normFactor(11,l,nu,&n);
    Tlmn.im = 0.0;
    Tlmn.re = 0.0;
    for (m=0; m<=l; m+=4)
    {
        S = Slmn(l,m,n,phi1,PHI,phi2);
        Tlmn.re += B[l][m/4][mu] * S.re;
    }
    Tlmn.re *= (En * sqt2PI);
    return Tlmn;
}
/* -----
* This function calculates the T functions cubic-cubic symmetry (Bunge eqn. (14.271)).
* -----
complex CubCubicT(int l,int mu,int nu,float phi1,float PHI,float phi2)
{
    complex Tlmn,S;
    int      m,n;
    Tlmn.im = Tlmn.re = 0.0;
    for (m=0; m<=l; m+=4) for(n=0; n<=l; n+=4)
    {
        S = Slmn(l,m,n,phi1,PHI,phi2);
        Tlmn.re += B[l][m/4][mu] * B[l][n/4][nu] * S.re;
    }
    Tlmn.re *= (2 * PI);
    return Tlmn;
}

/* -----
* This function calculates the T functions when both symmetries are triclinic.
* -----
complex TriTriclT(int l,int mu,int nu,float phi1,float PHI,float phi2)
{
    complex Tlmn;
    int      nup,mup;
    nup = TriMap(nu);
    mup = TriMap(mu);
    Tlmn = noSymT(l,mup,nup,phi1,PHI,phi2);
    return Tlmn;
}

```

Appendix H : Property.h subroutine

Property.h

```
/* This file contains all of the subroutines for property_C.c*/  
  
#include<stdio.h>  
#include<stdlib.h>  
#include<math.h>  
  
/* Compute the Kronecker Delta function*/  
int Kdelta(int x, int z)  
{  
    int exit = 0;  
    if( x == z)  
        exit = 1;  
    else  
        exit = 0;  
    return exit;  
}  
  
/* Compute the Aijkm function for the Kp function*/  
double Aijkm(int i, int j, int k, int m, double C112, double C144)  
{  
    double temp = 0.0;  
    temp = (C112 * Kdelta(i,j) * Kdelta(k,m)) + C144 * (Kdelta(i,k) * Kdelta(j,m) + Kdelta(i,m) *  
    Kdelta(j,k));  
    return temp;  
}  
  
/* Compute the Bijkm function for the Kp function*/  
double Bijkm(int i, int j, int k, int m, double C112, double C144, double C212, double C244)  
{  
    double temp = 0.0;  
    temp = (C212 - C112) * (Kdelta(i,j) * Kdelta(k,m)) +  
    (C244 - C144) * (Kdelta(i,k) * Kdelta(j,m)) +  
    (C244 - C144) * (Kdelta(i,m) * Kdelta(j,k));  
    return temp;  
}  
  
/* Compute the gir values */  
double Gir(int i, int r, double phi1, double PHI, double phi2)  
{  
    double temp = 0.0;  
    if(i == 1)  
        if (r == 1)  
            /*      g[1][1]      */      temp      =      cos(phi1)*cos(phi2)      -  
            sin(phi1)*sin(phi2)*cos(PHI);  
        else  
            if(r == 2)
```

```

sin(phi1)*cos(phi2)*cos(PHI);
else
    /* g[1][2] */ temp = -cos(phi1)*sin(phi2) -
/* g[1][3] */ temp = sin(phi1)*sin(PHI);
else
    if(i == 2)
        if(r == 1)
            /* g[2][1] */ temp = sin(phi1)*cos(phi2) +
cos(phi1)*sin(phi2)*cos(PHI);
        else
            if(r == 2)
                /* g[2][2] */ temp = -sin(phi1)*sin(phi2) +
cos(phi1)*cos(phi2)*cos(PHI);
            else
                /* g[2][3] */ temp = -cos(phi1)*sin(PHI);
    else
        if(r == 1)
            /* g[3][1] */ temp = sin(phi2)*sin(PHI);
        else
            if(r == 2)
                /* g[3][2] */ temp = cos(phi2)*sin(PHI);
            else
                /* g[3][3] */ temp = cos(PHI);

return temp;
}

```